Enhanced Correlation of SMART Active Flap Rotor Loads

Sesi Kottapalli

Flight Vehicle Research and Technology Division
NASA Ames Research Center
Moffett Field, California
Sesi.B.Kottapalli@nasa.gov

   This is a follow-on study to a 2010 correlation effort. Measured data from the SMART rotor test in the NASA Ames 40- by 80- Foot Wind Tunnel are compared with CAMRAD II calculations. As background, during the wind tunnel test, unexpectedly high inboard loads were encountered, and it was hypothesized at that time that due to changes in the flexbeams over the years, the flexbeam properties used in the analysis needed updating. Boeing Mesa, recently updated these properties. This correlation study uses the updated flexbeam properties. Compared to earlier studies, the following two enhancements are implemented: i) the inboard loads (pitchcase and flexbeam loads) correlation is included for the first time (reliable prediction of the inboard loads is a prerequisite for any future anticipated flight-testing); ii) the number of blade modes is increased to better capture the flap dynamics and the pitchcase-flexbeam dynamics. Also, aerodynamically, both the rolled-up wake model and the more complex, multiple trailer wake model are used, with the latter slightly improving the blade chordwise moment correlation. This sensitivity to the wake model indicates that CFD is needed. Three high-speed experimental cases, one uncontrolled free flap case and two commanded flap cases, are considered. The two commanded flap cases include a 2° flap deflection at 5P case and a 0° flap deflection case. For the free flap case, selected modifications to the HH-06 section flap airfoil pitching moment table are implemented. For the commanded 2° flap case, the experimental flap variation is approximately matched by increasing the analytical flap hinge stiffness. This increased flap hinge stiffness is retained for the commanded 0° flap case also, which is treated as a free flap case, but with larger flap hinge stiffness. The change in the mid-span and outboard loads correlation due to the updating of the flexbeam properties is not significant. Increasing the number of blade modes results in an effective, commanded flap hinge stiffness of 4X baseline, not 3X as reported earlier. The inboard loads correlation is reasonable, but needs further study. Overall, the free flap case correlation is reasonable, thus confirming the basic correctness of the current semi-empirical modifications; the correlation for the commanded 2° flap at 5P case and the 0° flap case is also reasonable.

Nomenclature

c_m	=	pitching moment coefficient
C_T	=	helicopter thrust coefficient
HPP	=	half peak-to-peak
KTEF	=	flap hinge stiffness, ft-lb/rad
M	=	Mach number
MTW	=	multiple trailer wake
NP	=	integer (N) multiple of rotor speed
Per rev	=	per revolution
RmPtn	=	NASA wind tunnel Run "m" Point "n"
RW	=	rolled-up, single tip vortex wake
α	=	angle of attack
$α_s$	=	rotor shaft angle

μ	=	rotor advance ratio
σ	=	rotor solidity ratio

Sign Convention

Chordwise moment, + tip toward trailing edge.
Flap deflection, + trailing edge down.
Flatwise moment, + tip up.
Pitch link load, + in tension.
Torsion moment, + leading edge up.

I. Introduction

In 2008, DARPA, Boeing, the U.S. Army, and NASA completed a full-scale wind tunnel test of the Boeing Smart Material Advanced Rotor Technology (SMART) bearingless rotor, Refs. 1-2. The data from this wind tunnel test has been and is being used in several parallel attempts to validate the Helicopter Quieting Program noise prediction tools as well as to improve NASA's ability to predict rotor performance, vibration, and loads. The SMART rotor is a next generation rotor system that offers high bandwidth on-blade active trailing edge flaps that will provide unique modeling challenges for the vibration and noise prediction tool sets. Reference 3 contains a description of the SMART rotor.

This analytical work is a follow-on study to Refs. 4-5. Unlike these prior studies, the current study uses different, more representative nomenclature. An "open loop" condition in which the experimental flap actuator is not active (free flap condition) is now identified as a "free flap" condition. Thus, the "open loop" case of Ref. 5 is now called the "free flap" case. Similarly, a "closed loop" case in which the experimental flap actuator is activated to maintain a commanded azimuthal variation is now called a "commanded flap" case. To reiterate, except where necessary, this study uses the "free flap" and "commanded flap" terminology (instead of the "open loop" and "closed loop" terminology that was used in earlier studies).

Reference 4 considered the high-speed condition and Ref. 5 considered both low-speed and high-speed conditions. The current study uses updated flexbeam properties, explained as follows. As background, it was found during the SMART wind tunnel test that the inboard torsion loads were significantly higher than expected and were limiting the test conditions that could be achieved. The flexbeams used in the 2008 SMART wind tunnel test, Refs. 1-2, have higher torsion stiffness compared to those used in the 1992 MDART wind tunnel test, Refs. 6-9. The current flexbeam torsion stiffness is higher both due to an increase in its thickness and the addition of wrappings (the 1992 MDART flexbeams were unwrapped), and this led Boeing Mesa, to recently measure the SMART rotor blade flexbeam stiffnesses. The updated flexbeam stiffness data is documented in a January 2010 Boeing Technical Report by Straub, et al. This correlation study uses the updated flexbeam properties. Finally, compared to Ref. 5, the following two enhancements are implemented:

  i)   Correlation of the inboard loads is included, for the first time. Inboard loads were not considered in Ref. 5 that included only the mid-span and outboard blade loads (and the pitch link load). The current study additionally includes prediction of the pitchcase and flexbeam loads. As noted above, the inboard loads were of concern during the wind tunnel test, and must be reliably predicted prior to any future anticipated flight-testing. The inboard loads depend on the flexbeam and pitchcase properties and also on the hub-flexbeam-pitchcase geometry, with the flexbeam bending-torsion couplings playing an important role.

  ii) More blade modes are used in the rotor trim procedure for two reasons: a) to better capture the flap dynamics (improved modeling accuracy). This enhancement is important for the commanded flap cases where the analytical flap stiffness KTEF is increased to simulate a prescribed azimuthal flap deflection pattern; and b) to better capture the pitchcase-flexbeam dynamics. Fifteen blade modes were used in Ref. 5 and 40 blade modes are used in the current study.

Also, aerodynamically, whereas only the rolled-up wake model was used in Ref. 5, both the rolled-up wake model and the multiple trailer wake model are used in the current study. It was found that the multiple trailer wake model gives slightly improved half peak-to-peak blade chordwise bending moments, results shown later.

Three high-speed cases are considered, Table 1. For the first case, a free flap case with baseline KTEF (wind tunnel open loop condition), the airfoil tables are improved by introducing modifications to the flap airfoil tables at transonic Mach numbers. For the second case, a commanded 2° at 5P flap case (wind tunnel closed loop condition), in order to approximately match the test flap deflection, the effect of the SMART flap's piezoelectric actuator in its active state is modeled by an appropriate increase in the analytical KTEF. The third case, a commanded 0° flap case (wind tunnel closed loop condition), is subsequently treated as a free flap case, but with increased KTEF. Overall, this work considers two types of analytical models that involve the flap aerodynamics and separately, the flap stiffness. A fixed, rigid hub is considered, i.e. fuselage effects are not included. The rotorcraft comprehensive analysis CAMRAD II (Refs. 10-12) is used.

II. Measured Wind Tunnel Data

References 1-2 contain descriptions of the SMART Rotor test in the NASA Ames 40- by 80- Foot Wind Tunnel. The wind tunnel data used in this paper is taken from Ref. 1.

III. Results

Table 1 shows the three high-speed cases, $\mu = 0.30$, that have been studied. The corresponding wind tunnel run and point numbers are also shown in Table 1; Run 57, Point 33 (R57Pt33) is an open loop (free flap) condition, and both the Run 46 points, R46Pt92 and R46Pt94, are closed loop (commanded flap) conditions.

A. Analytical Model

The CAMRAD II analytical model used is described briefly. The SMART rotor blade and flexbeam are modeled using elastic beam elements, with each element having two elastic flap bending, two elastic lag bending, and two torsion degrees of freedom. The blade consists of four beam elements, the torque tube one element, and the flexbeam three elastic elements, plus a rigid segment at the root end of the flexbeam, discussed as follows.

In Ref. 5, the flexbeam was modeled with rigid elements at each of its ends (the root and the pitchcase-flexbeam attachment location), and 15 blade modes were used in the rotor trim procedure. In the current study, it was found that the inboard loads prediction needed improvement, especially the flexbeam torsion moment that was consistently overpredicted and the pitchcase flatwise moment that was consistently underpredicted. To improve this correlation, the effect of an elastic pitchcase-flexbeam attachment was studied. Also, in order to better capture the pitchcase-flexbeam dynamics, the number of blade modes was increased to 40. To summarize, without presenting detailed results, it was found that, compared to a rigid pitchcase-flexbeam attachment, an elastic pitchcase-flexbeam attachment gave slightly better results; for all three high-speed cases under consideration, the overpredicted flexbeam torsion moment decreased by approximately 4% with all other inboard loads changing by smaller amounts. The results in this paper are based on an analytical model with an elastic pitchcase-flexbeam attachment and 40 blade modes (the number of blade modes was also increased for a second reason, flap dynamics, discussed later under *Flap Model*).

The following two free wake models were used: the rolled-up wake model, with single tip vortex and single circulation peak (RW model, used in Refs. 4-5) and the more complex, multiple trailer wake model with consolidation, compression form (MTW model, used in Refs. 5 and 13). It was found in the current study that the MTW model results in slightly better half peak-to-peak blade chordwise bending moments, results shown later (Figs. 2g-2h, 3h-3i, and 4h-4i). In order to further improve this correlation, a limited parametric study was conducted for the basic, 0° deg flap case in which the following two MTW model parameters were varied: the tip vortex core size and the time constant factor that determines the consolidation rate of the trailed vortex lines. It was found that the core size did not have a significant effect whereas the time constant factor had a significant effect; the usually underpredicted blade chordwise bending moment increased when the time constant factor was doubled, thus improving the correlation. However, detailed wake measurements for the SMART rotor that would produce an appropriate estimate of the time constant factor are not available. Thus, in the absence of experimental wake data, a

change to the current default time constant factor just to get improved correlation was considered somewhat arbitrary and was not done. The baseline, generic MTW model parameters were therefore retained. The flap extends from 0.74R to 0.92R. The aerodynamic model used 20 spanwise panels for the entire blade, 10 inboard of the flap, 6 on the flap (from 0.74R to 0.92R), and 4 outboard of the flap.

Flap Model. The trailing edge flap was modeled as a rigid body, using the measured flap hinge stiffness KTEF, flap hinge damping, and flap mass. The actual flap tested in the wind tunnel was mounted to the blade using five equally spaced hinges to minimize stresses. In the current study, the rigid flap is modeled as having one attachment point, at the flap mid-span, through which the flap loads are transmitted to the blade in a concentrated manner. Also, in the context of active control theory and practice, the current approach represents an open loop simulation in which the flap is free to respond dynamically (with prescribed spring stiffness, damping, mass, and inertia) to the aerodynamic environment, and the commanded flap deflection works through the flap spring. The actual flap deflection includes its dynamic response. During the wind tunnel test, for those runs in which the closed loop controller, Ref. 2, was activated, a piezoelectric actuator provided an additional, time-varying actuation to maintain a prescribed flap deflection pattern around the azimuth. In this study, the ability of the closed loop piezoelectric actuator to maintain a prescribed flap deflection is simulated by increasing the flap hinge stiffness KTEF. Earlier, Ref. 4 had considered 1.5X and 2.0X increases in KTEF, but in that free flap effort the emphasis was on matching the blade mid-span torsion moment whereas in the current commanded flap effort, the objective is to match the prescribed flap deflection. For rotor trim, Ref. 5 used 15 blade modes and in the current study 40 modes are used to better capture the flap dynamics (improved modeling accuracy). This enhancement is important for the commanded flap cases. For the free flap case, the baseline value of KTEF is used.

Figure 1 shows the frequency fan plot using the updated flexbeam properties. At nominal RPM, there are no significant differences between the old and new frequencies except that the 2nd chordwise mode frequency has moved a little closer to 4P.

In the figures, the following legends are used:
"Predicted (Ref. 5), …"   refers to Ref. 5 results, details as follows:
   a)   pre 2010 flexbeam properties
   b)   15 blade modes
   c)   for flexbeam, rigid end connections
   d)   rolled-up wake (RW)
"Updated predicted, ..." refers to the current results, details as follows:
   a)   updated 2010 flexbeam properties
   b)   40 blade modes
   c)   for flexbeam, only root end connection rigid (elastic pitchcase-flexbeam attachment)
   d)   rolled-up wake and multiple trailer wake (MTW)

The legends for the free flap, baseline KTEF, figures contain "… HH-06 flap c_m modified", and this refers to the compressibility-related, high-speed modifications to the flap pitching moment airfoil table for the outboard HH-06 section, discussed in detail in Ref. 5. The HH-06 flap c_m has been modified for selected transonic Mach numbers. Also, "…, *n*X KTEF" refers to an *n*-times increase from the baseline flap hinge stiffness value of 81.52 ft-lb/rad.

B.   Free Flap, Baseline Flap Stiffness

Without getting into CFD-based loads calculations, compressibility effects are studied by modifications to the flap airfoil properties, Ref. 5. The final modifications and the resulting correlation are described as follows (baseline KTEF).

Mid-span, Outboard, and Pitch Link Loads. Figure 2a shows the azimuthal correlation for the blade torsion moment at 0.64R. The following three analytical variations are shown: i) earlier results from Ref. 5 using the rolled-up wake, RW, model; ii) the current, updated predictions using the RW model, and iii) the current, updated predictions using the multiple trailer wake, MTW, model. The HH-06 flap c_m modifications were described in detail in Ref. 5. Briefly, to improve the advancing blade torsion moment correlation, first, only the HH-06 flap airfoil tables are modified, and second, these modifications cover high Mach numbers, negative angles of attack, and positive flap deflection (the blade HH-06 airfoil tables are not modified). Figures 2a-2b show the resulting torsion moment correlation at

0.64R and 0.81R, respectively. The corresponding flatwise and chordwise bending moment correlations are shown in Figs. 2c-2f, at 0.59R and 0.81R, respectively.

The current and Ref. 5 results are essentially the same for the torsion and flatwise moments (for both RW and MTW models), Figs. 2a-2d; the corresponding chordwise moment correlation is slightly different, Figs. 2e-2f. Figures 2e-2f show that the MTW model slightly improves the chordwise moment correlation, and this can also be seen from Figs. 2g-2h that show the effect of the wake model on the current, half peak-to-peak loads (torsion, flatwise, chordwise, both mid-span and outboard). The aerodynamically more complex MTW model increases the usually underpredicted chordwise moment. This sensitivity to the wake model indicates that CFD is needed. The pitch link load correlation is shown in Fig. 2i, and the corresponding half peak-to-peak values are as follows: test, 75 lb and from the current analysis, 72 lb (RW) and 66 lb (MTW). Figure 2j compares the measured and predicted time-histories for flap 1. The current and Ref. 5 flap deflections are essentially the same; the corresponding pitch link load correlations are slightly different.

Inboard Loads. Figures 2k- 2p show the following inboard loads:
   i)   blade torsion moment at 0.25R, Fig. 2k
   ii)   pitchcase torsion moment at 0.13R, Fig. 2l
   iii) pitchcase flatwise moment at 0.16R, Fig. 2m
   iv)   pitchcase chordwise moment at 0.16R, Fig. 2n
   v)   flexbeam torsion moment at 0.13R, Fig. 2o
   vi)   flexbeam chordwise moment at 0.13R, Fig. 2p.
Overall, the current inboard loads correlation appears reasonable with the following exceptions: the pitchcase flatwise moment is underpredicted, Fig. 2m, and the flexbeam torsion moment is overpredicted, Fig. 2o.

To summarize, Figs. 2a-2p show that the current free flap correlation is fair, but the inboard loads correlation could be improved. Compared to the RW model, the MTW model gives slightly better blade chordwise moments.

C.   Commanded 2° at 5P Flap, Matched Deflection

Similar to the approach taken in Ref. 5, a parametric study was conducted varying the flap hinge stiffness KTEF with the objective of matching the test deflection time history for the commanded 2° flap at 5P case (Commanded Flap, Table 1). Figure 3a shows both the Ref. 5 results, 15 blade modes, and the current results, 40 blade modes, and clearly, the current improved modeling accuracy necessitates that the flap stiffness be raised to 4X baseline value (not 3X as used in Ref. 5). Figure 3a also shows that, compared to the Ref. 5 result, the current 4X result gives a slightly better match for the retreating side flap deflection as well.

The measured and predicted flap deflections for blade 1 are shown in Fig. 3a, discussed above. Figures 3b-3c show the resulting torsion moment correlation at 0.64R and 0.81R, respectively. The corresponding flatwise and chordwise bending moment correlations are shown in Figs. 3d-3g, at 0.59R and 0.81R, respectively. The effect of the wake model on the mid-span and outboard half peak-to-peak blade moments is shown in Figs. 3h-3i. The chordwise moment is substantially underpredicted. There could be a problem with the blade description. The pitch link load correlation is shown in Fig. 3j, and the corresponding half peak-to-peak values are as follows: test, 147 lb and from the current analysis, 148 lb (RW) and 149 lb (MTW). The current 4X results and the Ref. 5 results are essentially the same for the torsion and flatwise moments; the corresponding chordwise bending moment and the pitch link load correlations are slightly different, with the chordwise moment still underpredicted. Overall, Figs. 3b-3j show that the correlation is fair for torsion, poor for bending, with overprediction on the advancing side.

Figures 3k-3p show the *inboard results* as follows: blade torsion moment at 0.25R, pitchcase torsion moment at 0.13R, pitchcase flatwise and chordwise moments at 0.16R, and flexbeam torsion and chordwise moments at 0.13R, respectively. Overall, the inboard loads correlation appears reasonable with the following exceptions: the pitchcase flatwise moment, Fig. 3m, is underpredicted and the flexbeam torsion moment is overpredicted, Fig. 3o.

Overall, at this commanded 2° flap at 5P deflection condition, Figs. 3b-3p show that the correlation is fair for torsion, poor for bending, with overprediction on the advancing side, and also that the inboard loads correlation could be improved.

D. Commanded 0° Flap, Modeled as Free Flap with Increased Flap Stiffness

Figure 4a shows the measured and predicted flap deflections for blade 1. Figures 4b-4c show the torsion moment correlation at 0.64R and 0.81R, respectively. The corresponding flatwise and chordwise bending moment correlations are shown in Figs. 4d-4g, at 0.59R and 0.81R, respectively. The effect of the wake model on the mid-span and outboard half peak-to-peak blade moments is shown in Figs. 4h-4i, and overall, these trends are similar to the free flap with baseline KTEF case trends, Figs. 2g-2h. Similar to the first free flap case, this sensitivity to the wake model indicates that CFD is needed. The pitch link load correlation is shown in Fig. 4j, and the corresponding half peak-to-peak values are as follows: test, 56 lb and from the current analysis, 64 lb (RW) and 63 lb (MTW). The current 4X KTEF results and the Ref. 5 results are essentially the same for the torsion and flatwise moments; the corresponding chordwise bending moment and the pitch link load correlations are slightly different.

Figures 4k-4p show the *inboard results* as follows: blade torsion moment at 0.25R, pitchcase torsion moment at 0.13R, pitchcase flatwise and chordwise moments at 0.16R, and flexbeam torsion and chordwise moments at 0.13R, respectively. Overall, the inboard loads correlation appears reasonable with the following exceptions: the pitchcase flatwise moment, Fig. 4m, is underpredicted and the flexbeam torsion moment is overpredicted, Fig. 4o.

Overall, at this commanded flap 0° condition, Figs. 4a-4p show that the correlation is fair, but the inboard loads correlation could be improved.

IV. Conclusions

The prediction of SMART active trailing edge flap rotor loads, using updated flexbeam properties, was considered in this study. The following three high-speed, $\mu = 0.30$, experimental cases were considered for correlation:
  i)   Free flap (open loop)
  ii) Commanded flap with 2° flap deflection at 5P (closed loop)
  iii) Commanded flap with 0° flap deflection (closed loop)
Measured data from the NASA Ames 40- by 80- Foot Wind Tunnel were compared with CAMRAD II predictions.

It should be noted that, except where necessary, this study uses the "free flap" and "commanded flap" terminology (instead of the "open loop" and "closed loop" terminology used in earlier studies).

Compared to earlier studies, the following two enhancements were implemented: i) the inboard loads (pitchcase and flexbeam loads) correlation was included for the first time (reliable prediction of the inboard loads is a prerequisite for any future anticipated flight-testing); and ii) the number of blade modes was increased to better capture the flap dynamics for the commanded flap conditions and also to include higher frequency pitchcase modes. Also, aerodynamically, whereas only the rolled-up wake model was used previously, both the rolled-up wake model and the multiple trailer wake model were used in the current study. It was found that the multiple trailer wake model gave slightly improved half peak-to-peak blade chordwise bending moments, details below.

For the free flap condition (baseline flap hinge stiffness), selected modifications to the HH-06 flap airfoil pitching moment table were implemented; the correlation was reasonable, thus confirming the basic correctness of the current semi-empirical modifications. Since only the HH-06 section flap c_m was modified (for selected Mach numbers, blade angles of attack, and flap deflection), this study addressed only a limited portion of the SMART rotor airfoil table database. For the commanded flap conditions, the effect of the SMART flap actuator was modeled by increased flap hinge stiffness; the correlation was reasonable considering the relatively simple, first generation flap model that was used. Specific conclusions follow.

  1.   The change in the mid-span and outboard loads correlation due to the updating of the flexbeam properties was not significant; only the blade chordwise moment and pitch link load were slightly different, with the blade torsion and flatwise moments essentially unchanged.

2. In the current commanded flap simulation, use of an increased number of blade modes (improved modeling accuracy) resulted in an effective, commanded flap hinge stiffness of 4X baseline, not 3X as reported earlier.

3. Overall, the current inboard loads correlation was reasonable, but needs improvement (the pitchcase flatwise moment was underpredicted and the flexbeam torsion moment was overpredicted).

4. Previous studies have used the rolled up wake model for the high-speed, $\mu = 0.30$, cases under consideration. In the current study, the aerodynamically more complex multiple trailer wake, MTW, model was also tried out. Overall, the MTW model improved the blade chordwise moment correlation, and this sensitivity to the wake model indicates that CFD is needed.

5. The following conclusions refer to the mid-span and outboard loads:

   a. For the commanded 0° flap deflection case, the correlation was fair, but could be improved.

   b. For the commanded 5P, 2° flap case, the effect of the flap motion was reasonably captured. The correlation was fair for torsion, poor for bending, with overprediction on the advancing side.

   c. The pitch link load correlation was fair.

   d. Generally, the chordwise moments were underpredicted, and the MTW model increased the half peak-to-peak values, thus improving the correlation.

References

[1]Straub, F. K., Anand, V. R., Birchette, T. S., and Lau, B. H., "Wind Tunnel Test of the SMART Active Flap Rotor," American Helicopter Society 65th Annual Forum Proceedings, Grapevine, TX, May 27-29, 2009.

[2]Hall, S. R., Anand, V. R., Straub, F. K., and Lau, B.H., "Active Flap Control of the SMART Rotor for Vibration Reduction," American Helicopter Society 65th Annual Forum Proceedings, Grapevine, TX, May 27-29, 2009.

[3]Straub, F. K. and Anand, V.R., "Whirl Tower Test and Analysis of the SMART Material Actuated Rotor Technology (SMART) Active Flap Rotor," American Helicopter Society 63rd Annual Forum Proceedings, Virginia Beach, VA, May 1-3, 2007.

[4]Kottapalli, S., and Straub, F.K., "Correlation of SMART Active Flap Rotor Loads," American Helicopter Society 65th Annual Forum Proceedings, Grapevine, TX, May 27-29, 2009.

[5]Kottapalli, S., "Low-Speed and High-Speed Correlation of SMART Active Flap Rotor Loads," American Helicopter Society Aeromechanics Specialists' Conference, San Francisco, CA, January 20-22, 2010.

[6]Murrill, R.J., Hamilton, B.K., Anand, V.R., Lauzon, D.M., and Tuttles, B., "Bearingless Main Rotor Whirl Test: Design, Analysis, and Test Results," American Helicopter Society 49th Annual Forum Proceedings, St. Louis, MO, May 19-21, 1993.

[7]McNulty, M., Jacklin, S., and Lau, B., "A Full-Scale Test of the McDonnell Douglas Advanced Bearingless Rotor in the NASA Ames 40- by 80- Foot Wind Tunnel," American Helicopter Society 49th Annual Forum Proceedings, St. Louis, MO, May 19-21, 1993.

[8]Nguyen, K., McNulty, M., Anand, V., and Lauzon, D., "Aeroelastic Stability of the McDonnell Douglas Advanced Bearingless Rotor" American Helicopter Society 49th Annual Forum Proceedings, St. Louis, MO, May 19-21, 1993.

[9]Jacklin, S. J., Lau, B. H., Nguyen, K. Q., Smith, R. L., and McNulty, M.J., "Full-Scale Wind Tunnel Test of the McDonnell Douglas Five-Bladed Advanced Bearingless Rotor: Performance, Stability, Loads, Control Power, Vibration and HHC Data," American Helicopter Society, American Helicopter Society Aeromechanics Specialists Conference, San Francisco, CA, January 19-21, 1994.

[10]Johnson, W., "CAMRAD II, Comprehensive Analytical Model of Rotorcraft Aerodynamics and Dynamics," Johnson Aeronautics, Palo Alto, California, 1992-1999.

[11]Johnson, W., "Technology Drivers in the Development of CAMRAD II," American Helicopter Society Aeromechanics Specialists' Conference, San Francisco, CA, January 19-21, 1994.

[12]Johnson, W., "A General Free Wake Geometry Calculation for Wings and Rotors," American Helicopter Society 51st Annual Forum Proceedings, Ft. Worth, TX, May 9-11, 1995.

[13]Kottapalli, S., "Calculation of Hub Loads at Low Airspeeds with Active Control," American Helicopter Society 63rd Annual Forum Proceedings, Virginia Beach, VA, May 1-3, 2007.

Table 1. SMART rotor correlation cases, 123 knots.

Correlation Cases	Run, Point	C_T/σ	α_s	μ
Free Flap, Baseline KTEF (1X KTEF)	57, 33	0.074	-9.1^o	0.30
Commanded Flap, 2° at 5P, 4X KTEF	46, 92	0.080	-9.1^o	0.30
Free Flap, 4X KTEF	46, 94	0.080	-9.1^o	0.30

American Institute of Aeronautics and Astronautics
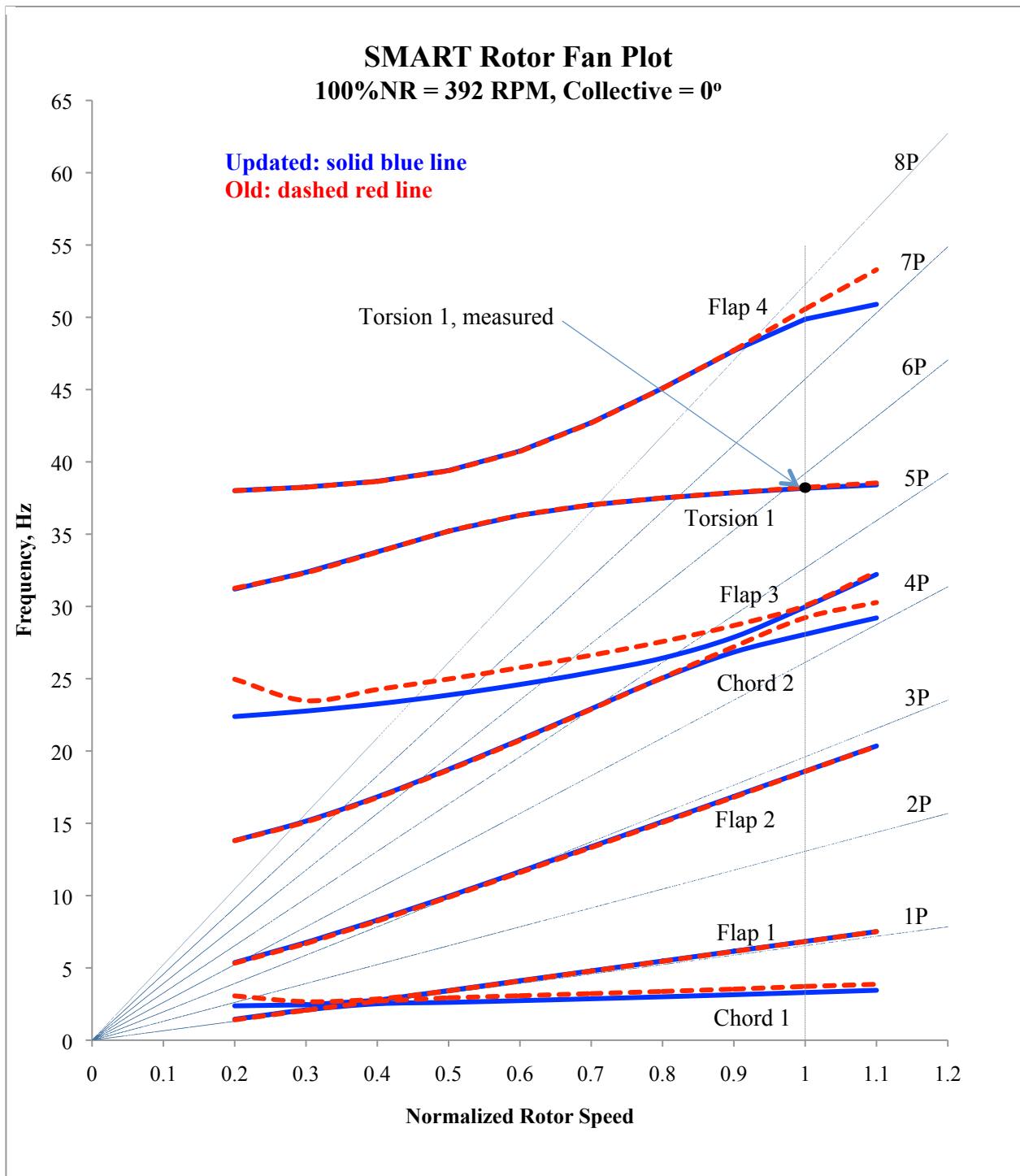
Fig. 1. SMART rotor fan plot (blade properties from January 2010 Boeing Technical Report by Straub, et al.).

American Institute of Aeronautics and Astronautics
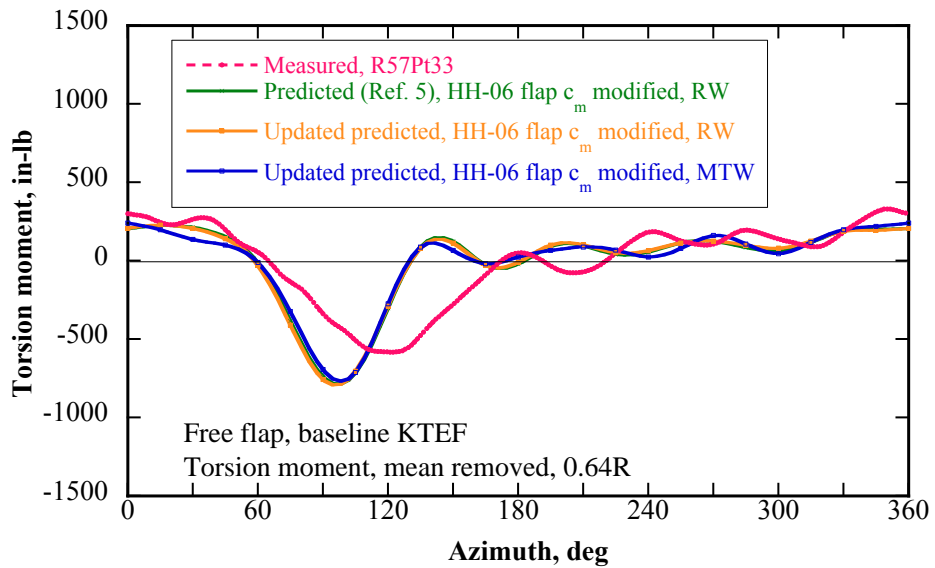
Fig. 2a. Torsion moment correlation, 0.64R, free flap, baseline KTEF.

Fig. 2b. Torsion moment correlation, 0.81R, free flap, baseline KTEF.

American Institute of Aeronautics and Astronautics
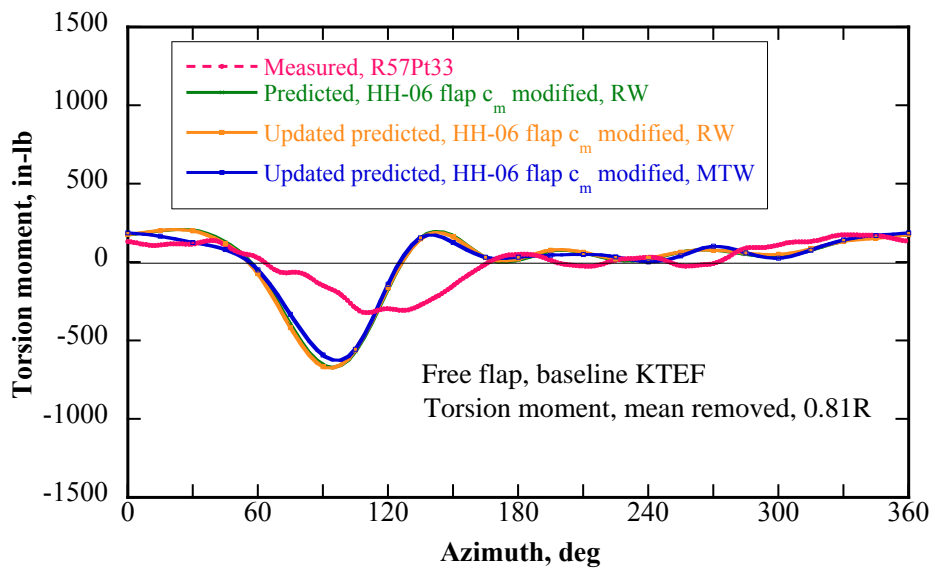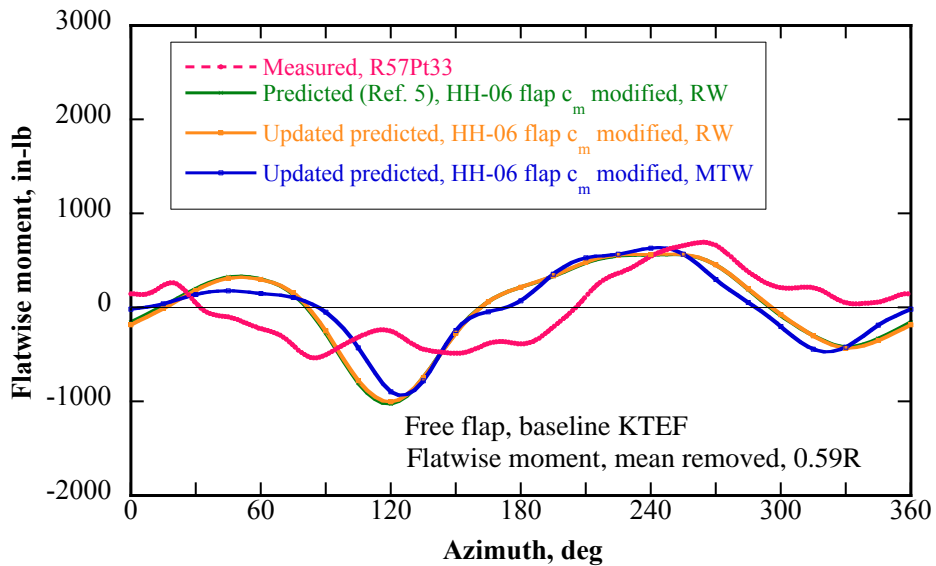
Fig. 2c. Flatwise bending moment correlation, 0.59R, free flap, baseline KTEF.

Fig. 2d. Flatwise bending moment correlation, 0.81R, free flap, baseline KTEF.

American Institute of Aeronautics and Astronautics
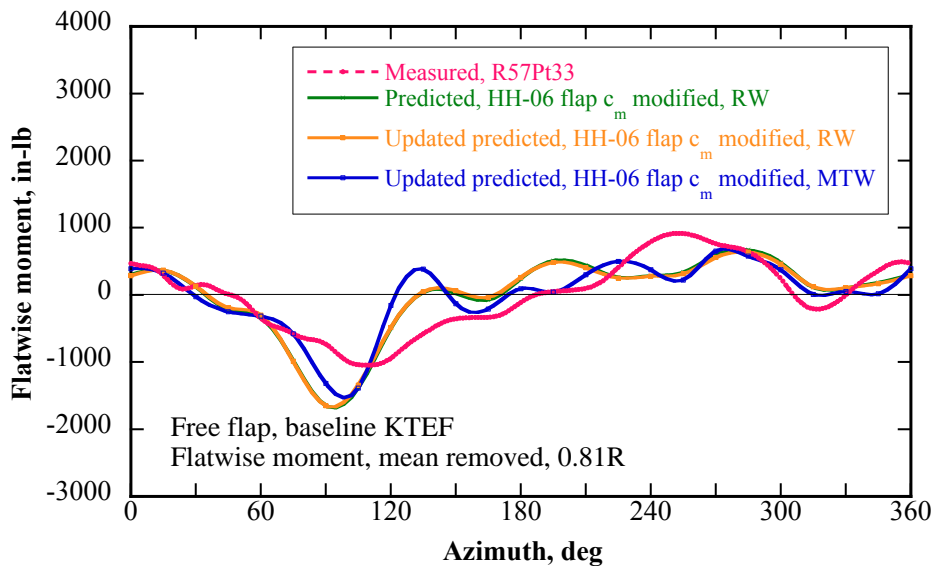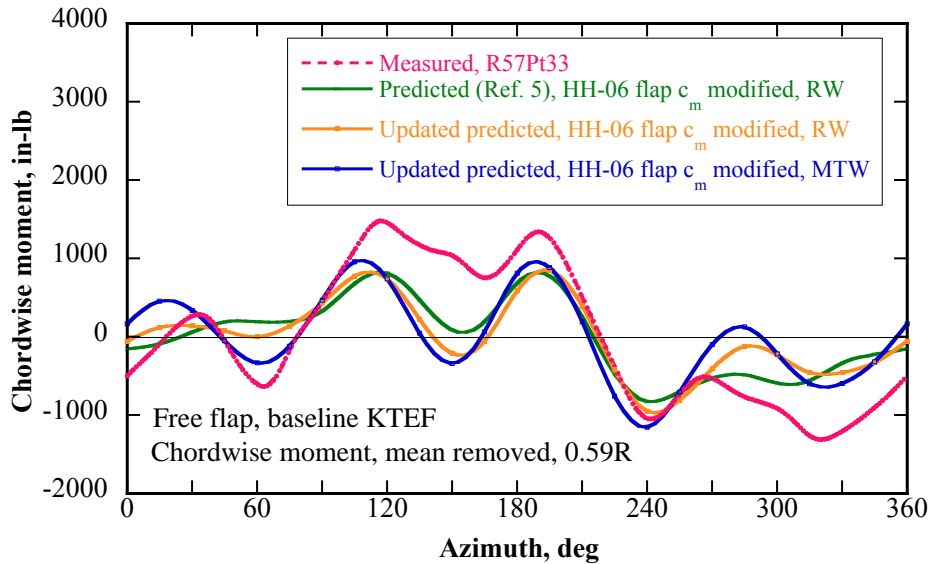
Fig. 2e. Chordwise bending moment correlation, 0.59R, free flap, baseline KTEF.
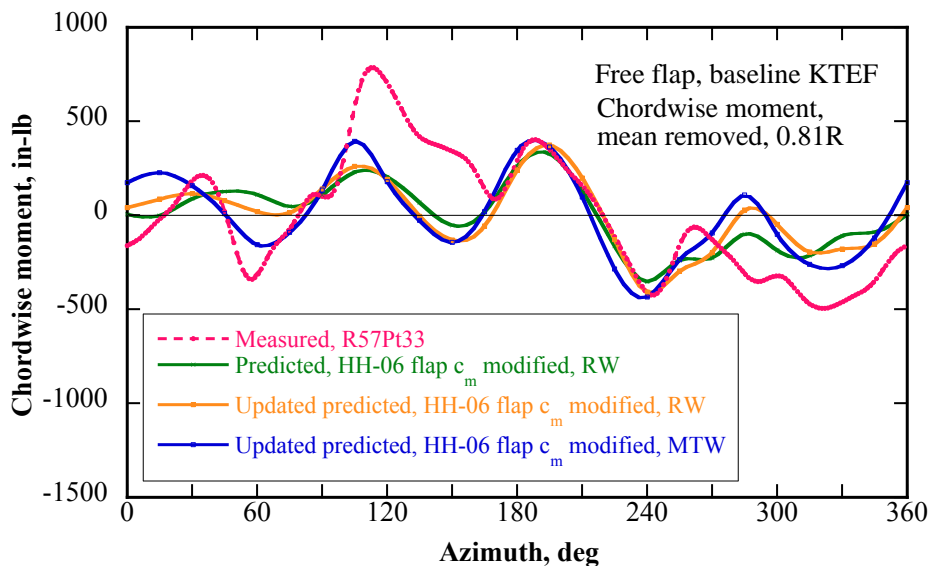
Fig. 2f. Chordwise bending moment correlation, 0.81R, free flap, baseline KTEF.
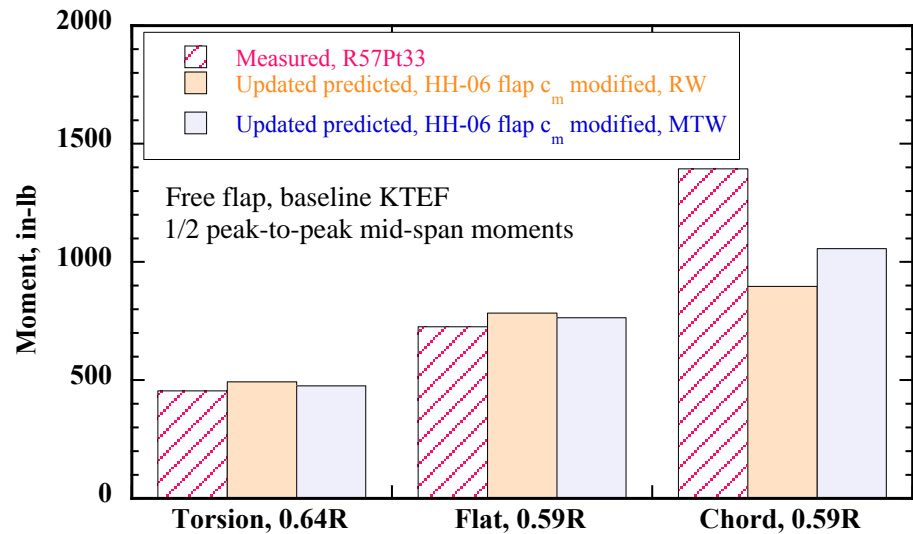
Fig. 2g. Mid-span moment correlation, free flap, baseline KTEF.

Fig. 2h. Outboard moment correlation, free flap, baseline KTEF.

American Institute of Aeronautics and Astronautics
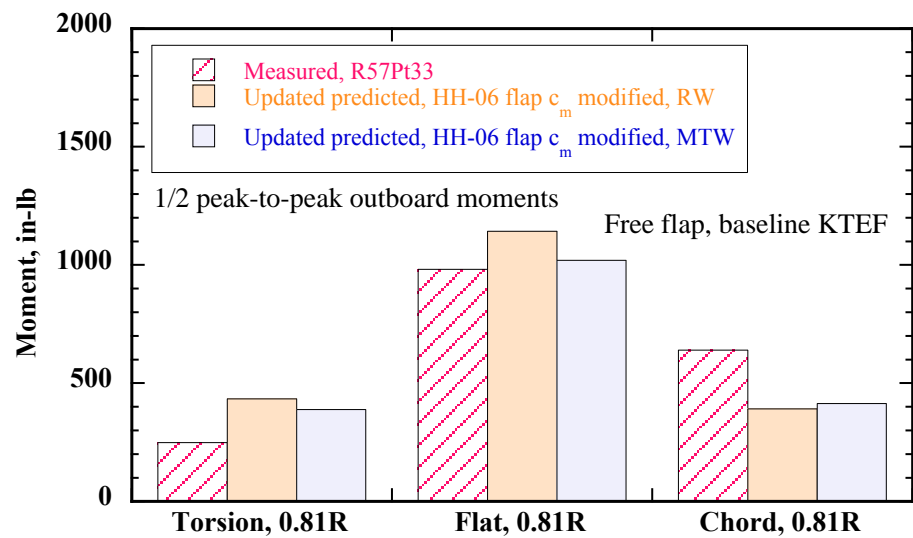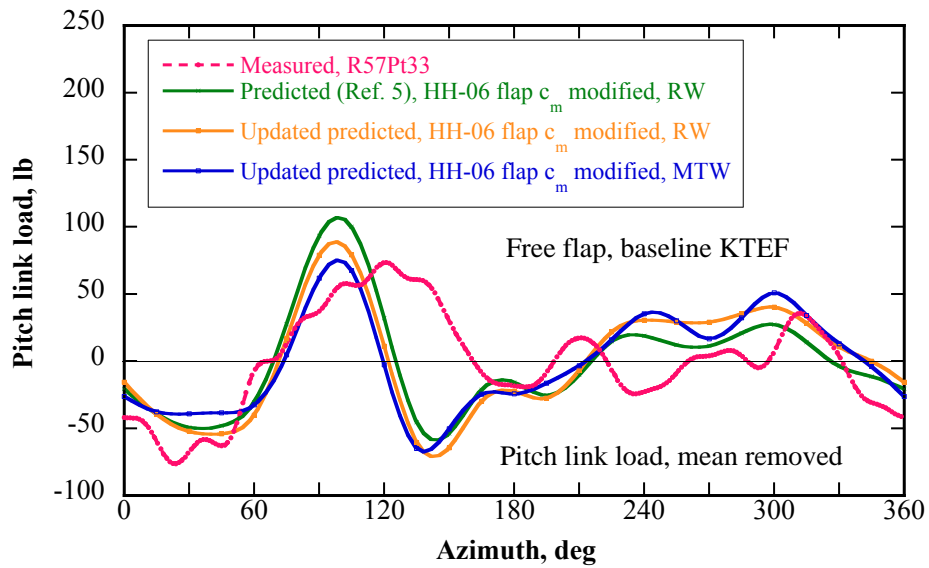
Fig. 2i. Pitch link load correlation, free flap, baseline KTEF.
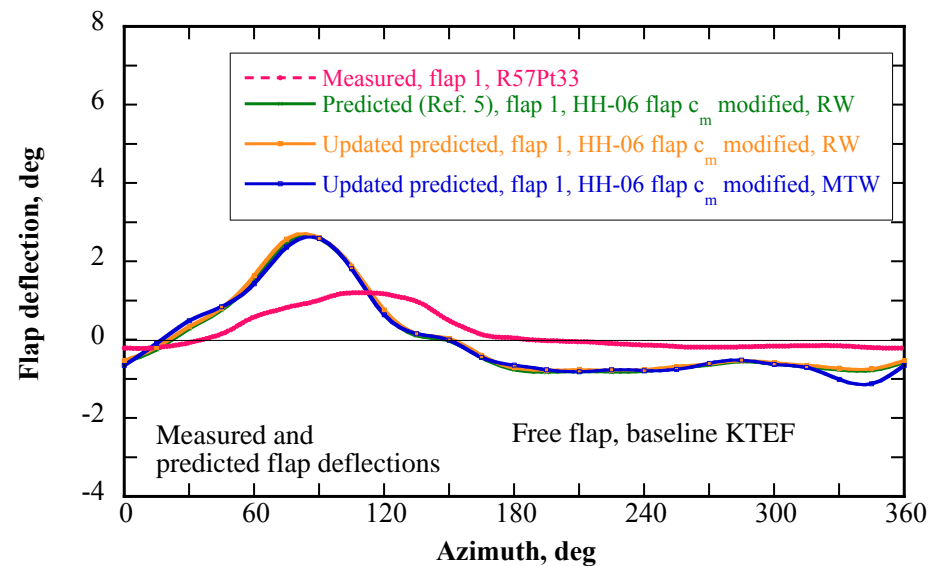
Fig. 2j. Measured and predicted flap deflections, free flap, baseline KTEF.

American Institute of Aeronautics and Astronautics
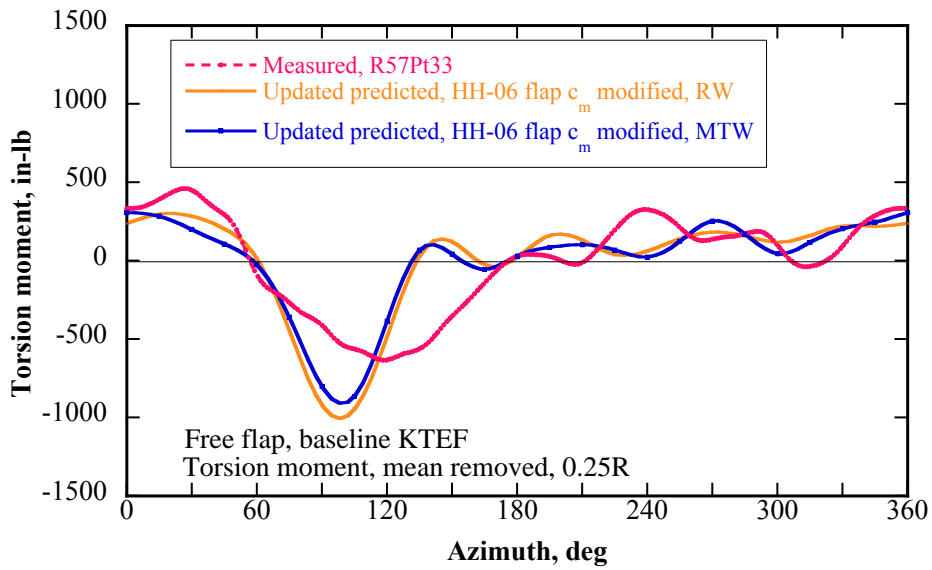
Fig. 2k. Inboard torsion moment correlation, 0.25R, free flap, baseline KTEF.
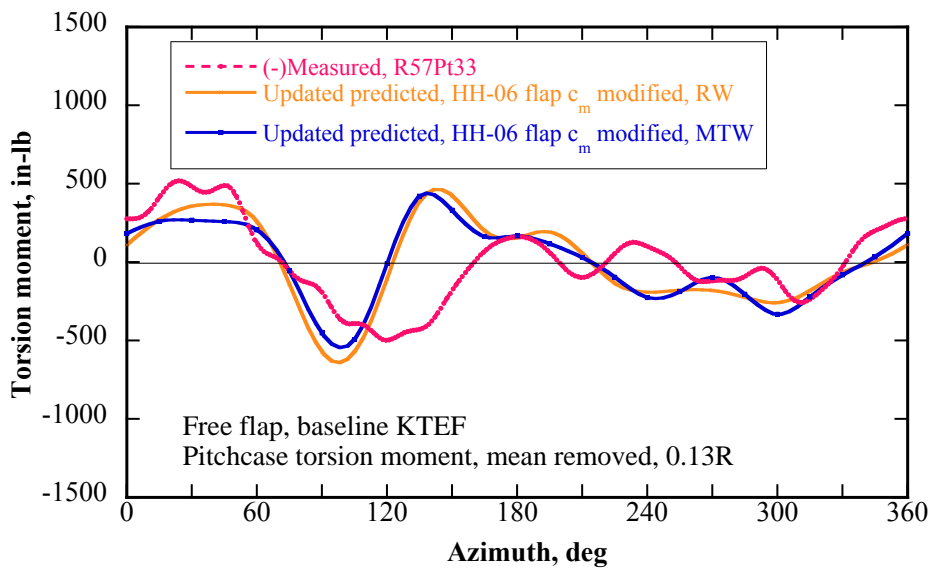
Fig. 2l. Pitchcase torsion moment correlation, 0.13R, free flap, baseline KTEF.

American Institute of Aeronautics and Astronautics
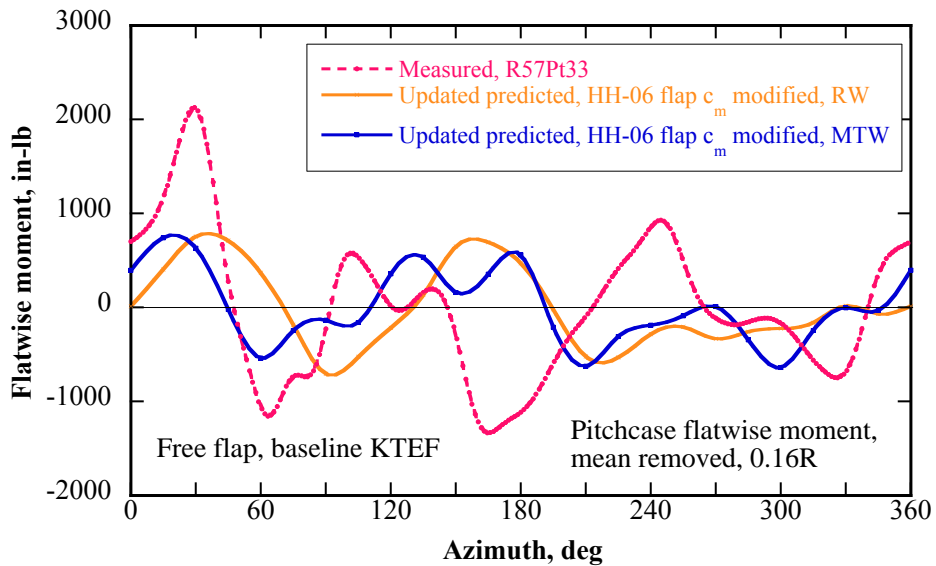
Fig. 2m. Pitchcase flatwise moment correlation, 0.16R, free flap, baseline KTEF.
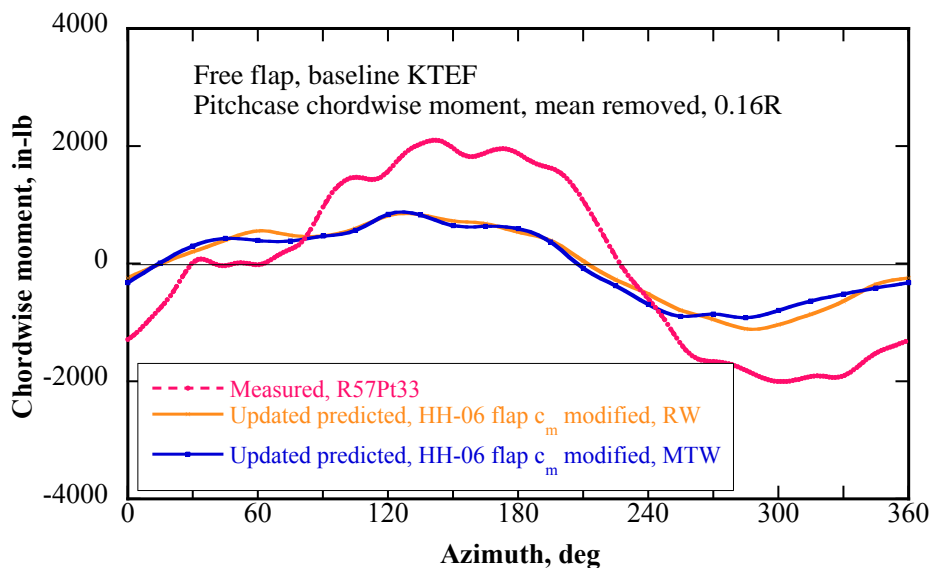
Fig. 2n. Pitchcase chordwise moment correlation, 0.16R, free flap, baseline KTEF.
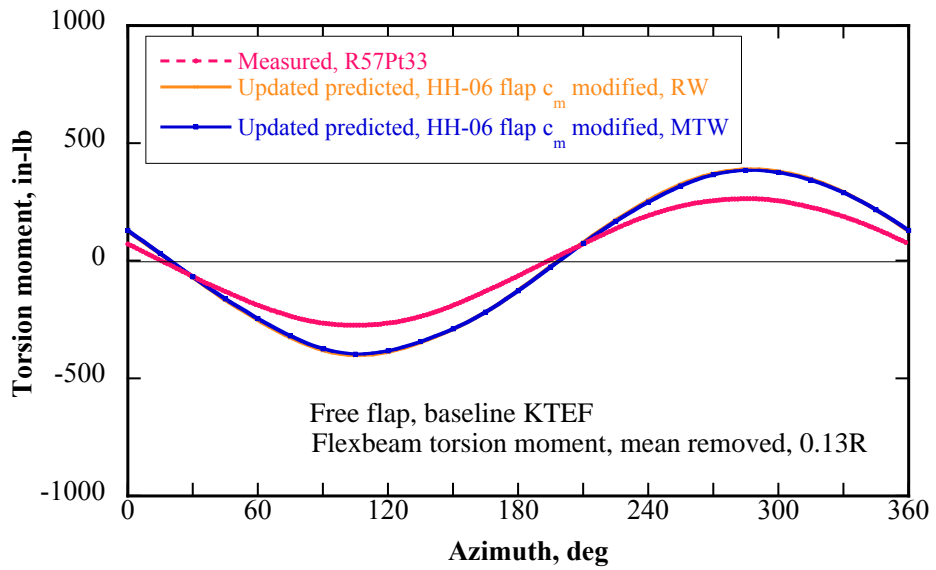
Fig. 2o. Flexbeam torsion moment correlation, 0.13R, free flap, baseline KTEF.
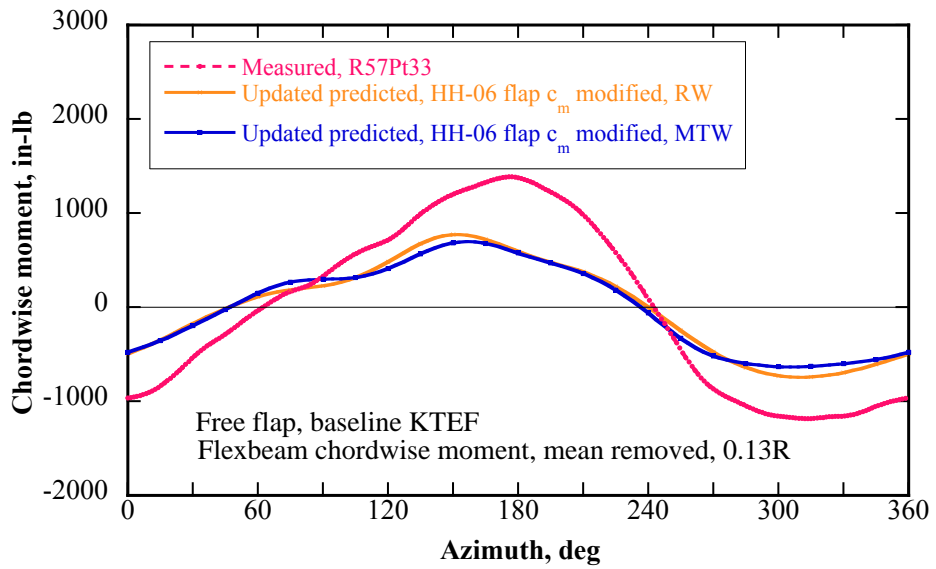
Fig. 2p. Flexbeam chordwise moment correlation, 0.13R, free flap, baseline KTEF.
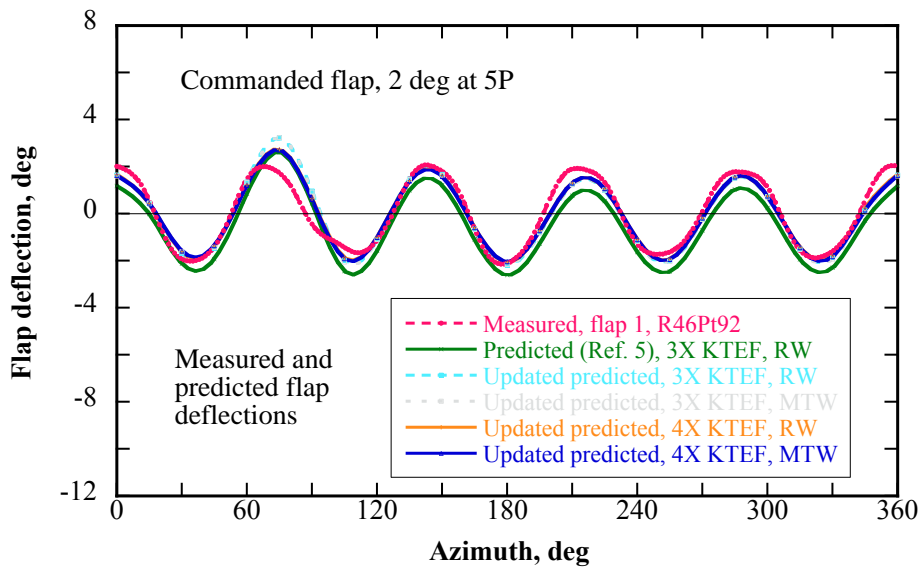
Fig. 3a. Measured and predicted flap deflections, commanded flap.
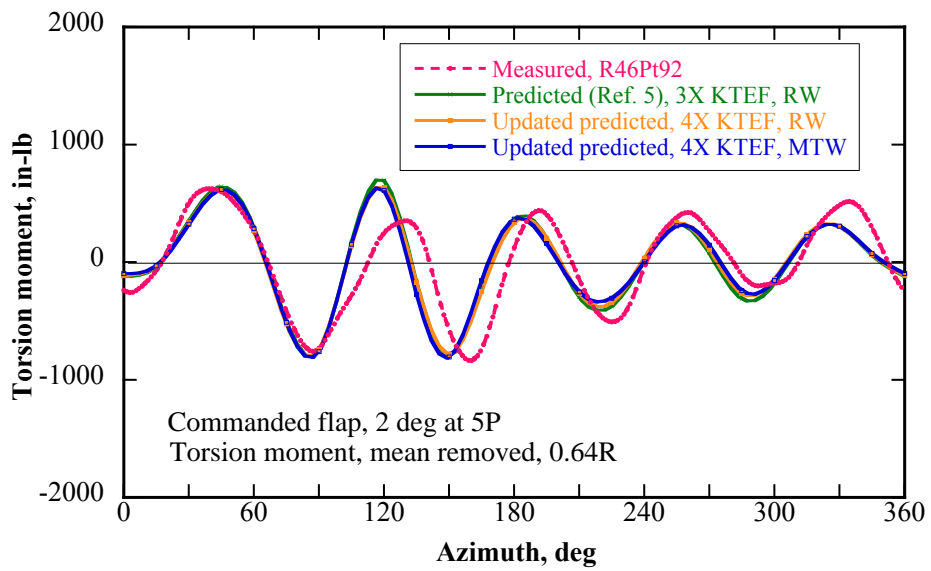
Fig. 3b. Torsion moment correlation, 0.64R, commanded flap.

American Institute of Aeronautics and Astronautics
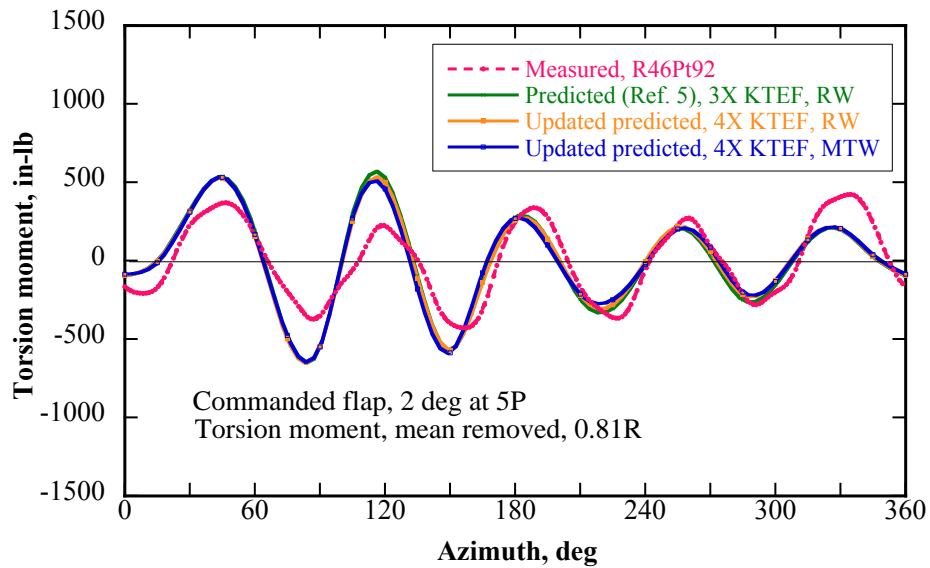
Fig. 3c. Torsion moment correlation, 0.81R, commanded flap.
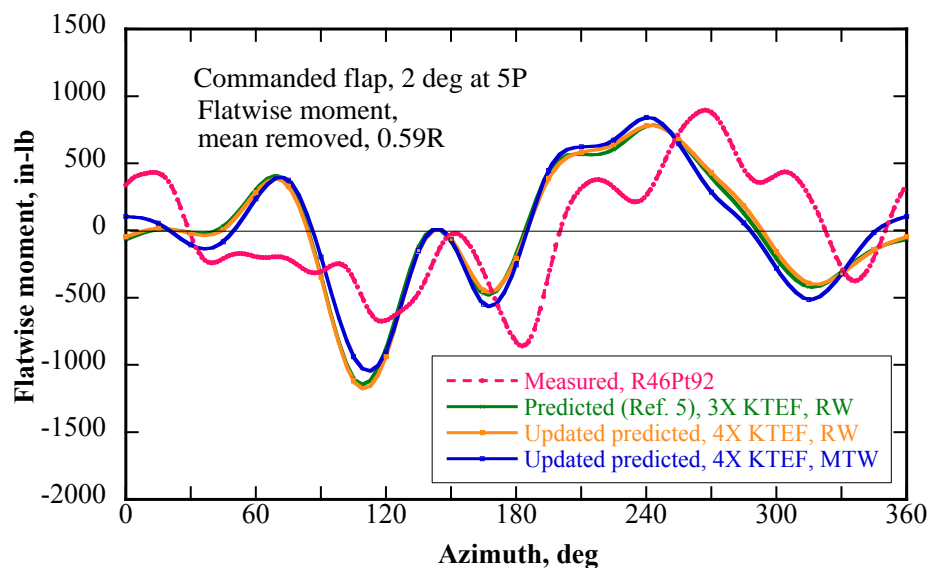
Fig. 3d. Flatwise bending moment correlation, 0.59R, commanded flap.
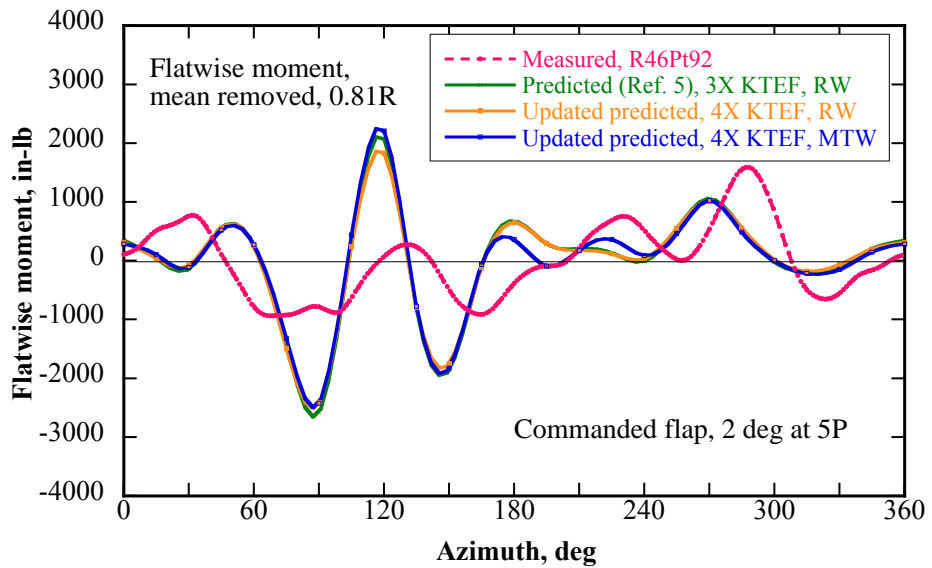
Fig. 3e. Flatwise bending moment correlation, 0.81R, commanded flap.
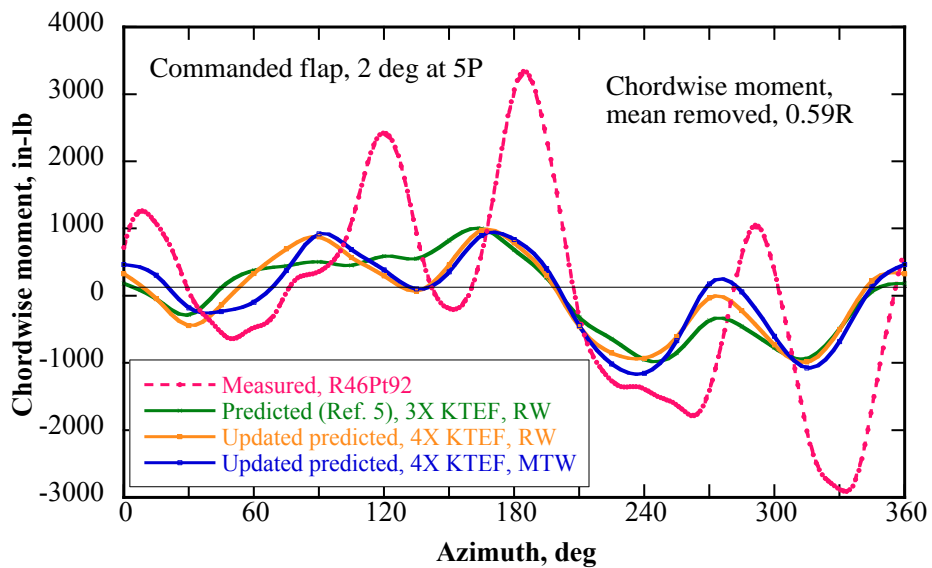
Fig. 3f. Chordwise bending moment correlation, 0.59R, commanded flap.
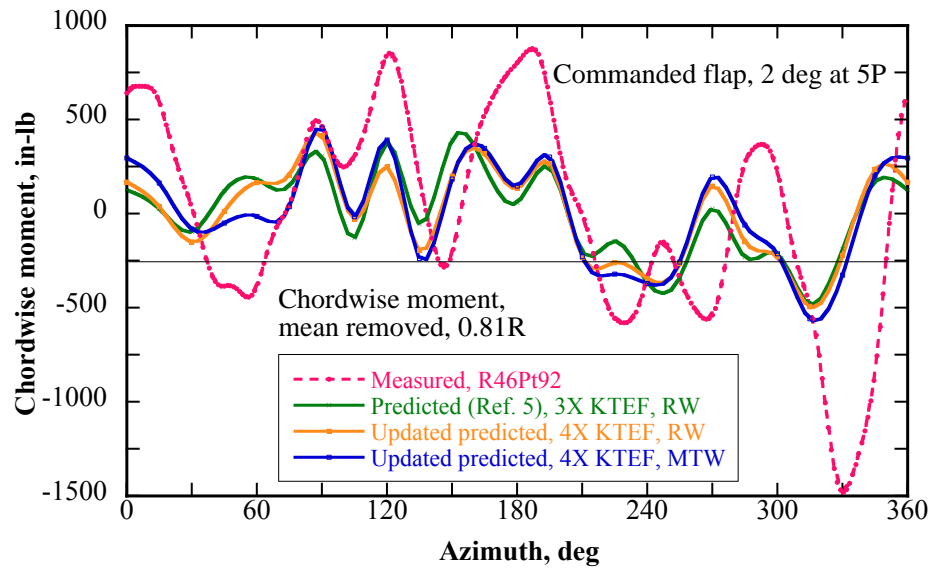
Fig. 3g. Chordwise bending moment correlation, 0.81R, commanded flap.
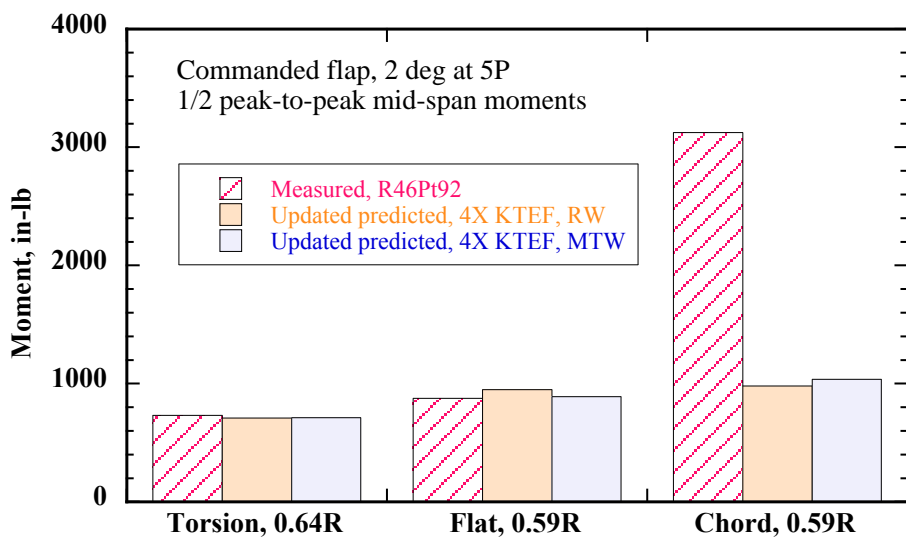
Fig. 3h. Mid-span moment correlation, commanded flap.
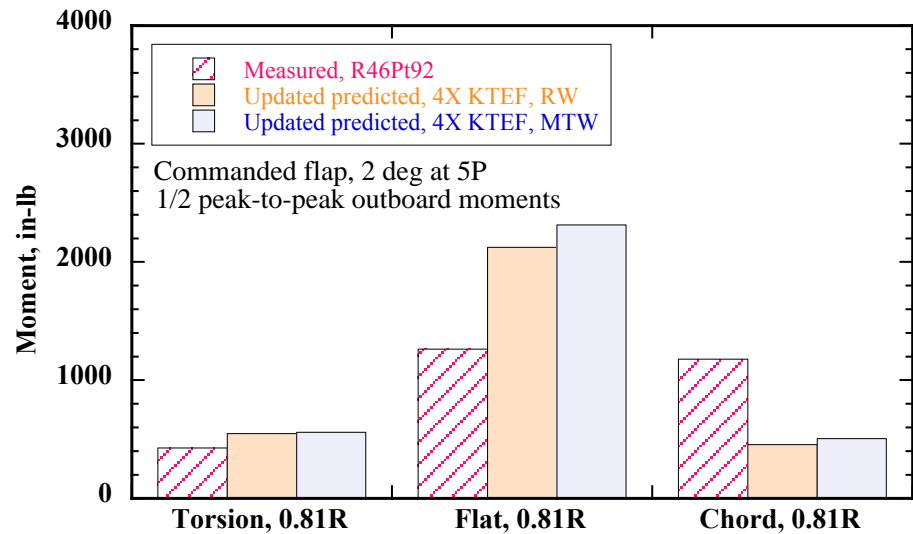
Fig. 3i. Outboard moment correlation, commanded flap.
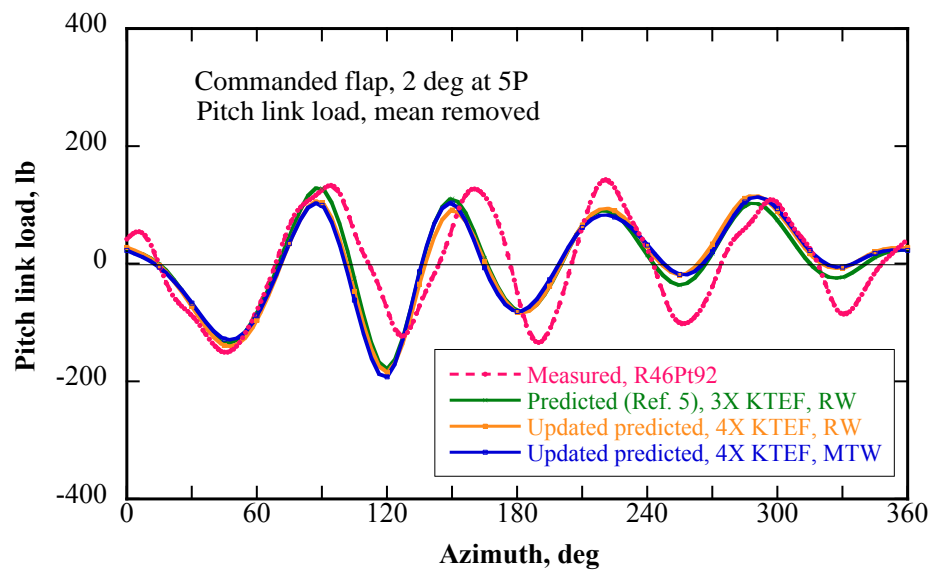
Fig. 3j. Pitch link load correlation, commanded flap.
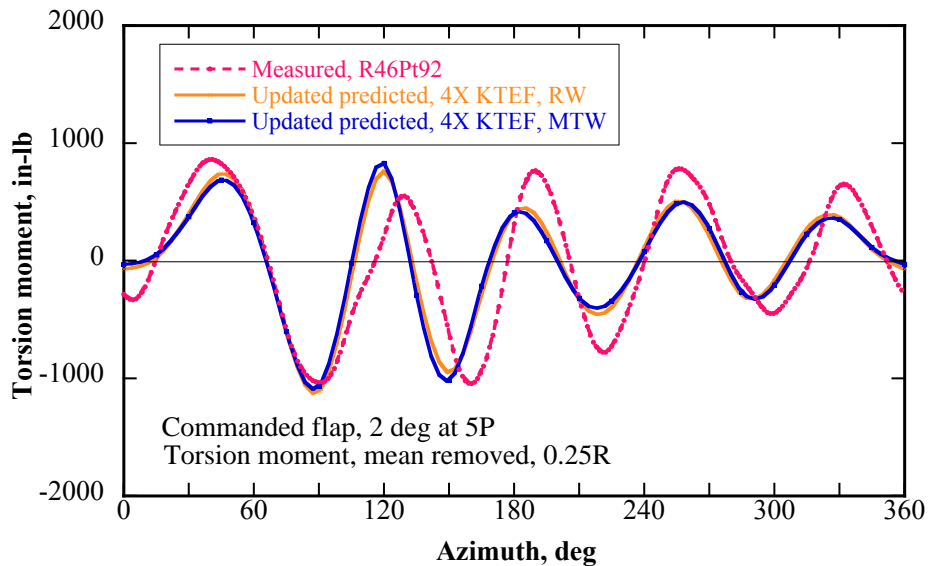
Fig. 3k. Inboard torsion moment correlation, 0.25R, commanded flap.
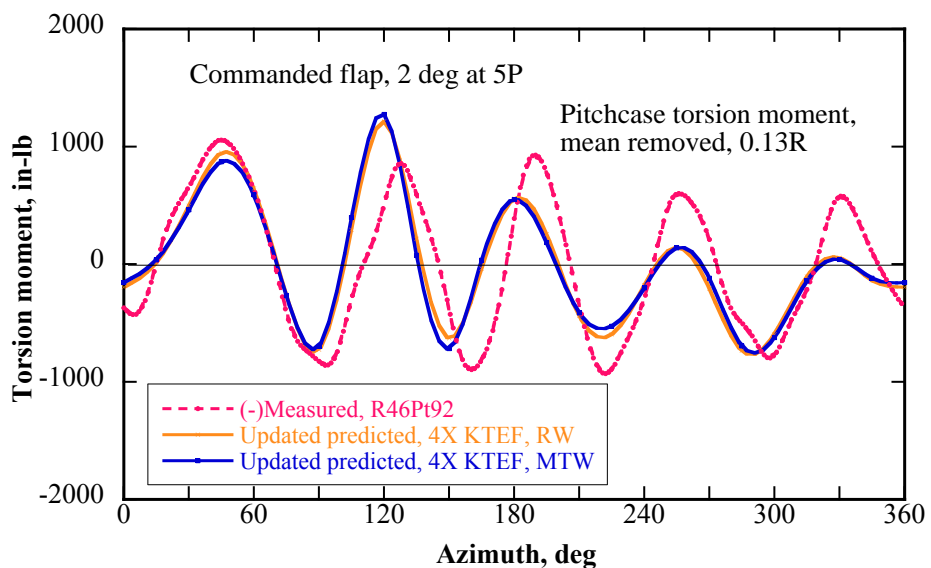
Fig. 3l. Pitchcase torsion moment correlation, 0.13R, commanded flap.
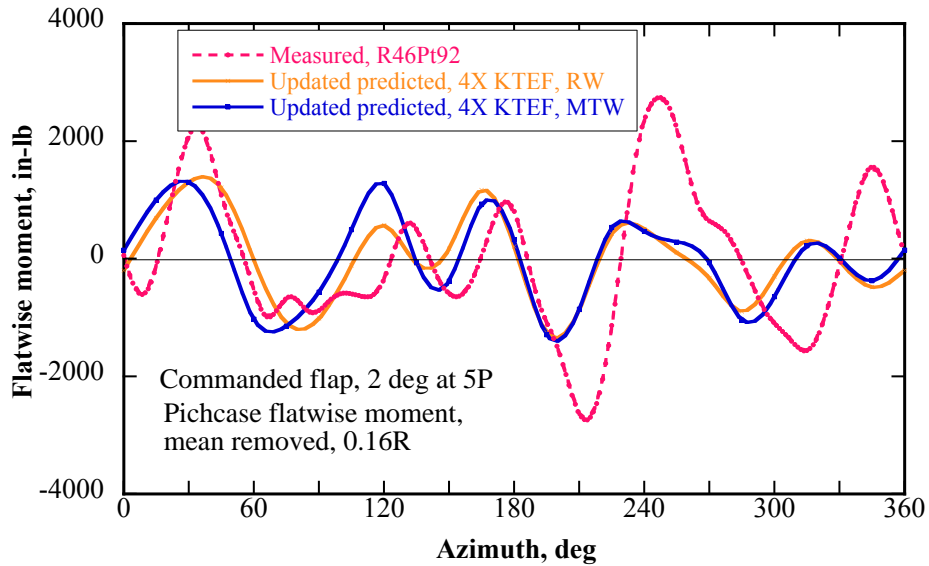
Fig. 3m. Pitchcase flatwise moment correlation, 0.16R, commanded flap.

Fig. 3n. Pitchcase chordwise moment correlation, 0.16R, commanded flap.

American Institute of Aeronautics and Astronautics
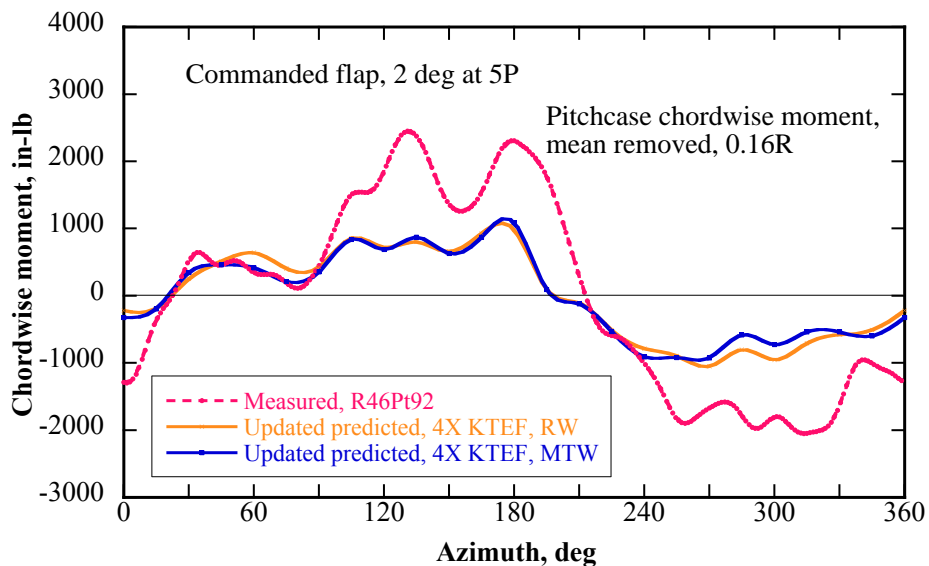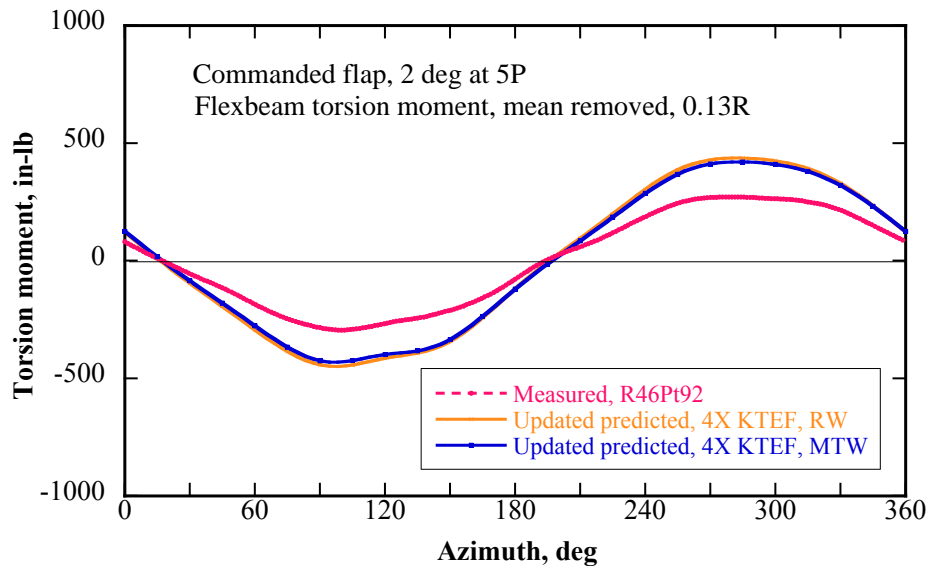
Fig. 3o. Flexbeam torsion moment correlation, 0.13R, commanded flap.
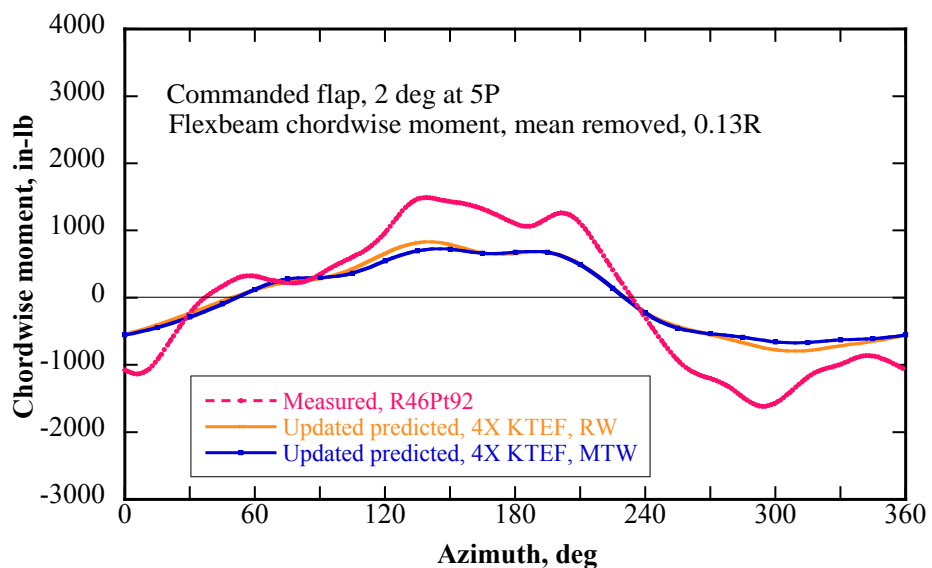
Fig. 3p. Flexbeam chordwise moment correlation, 0.13R, commanded flap.

American Institute of Aeronautics and Astronautics
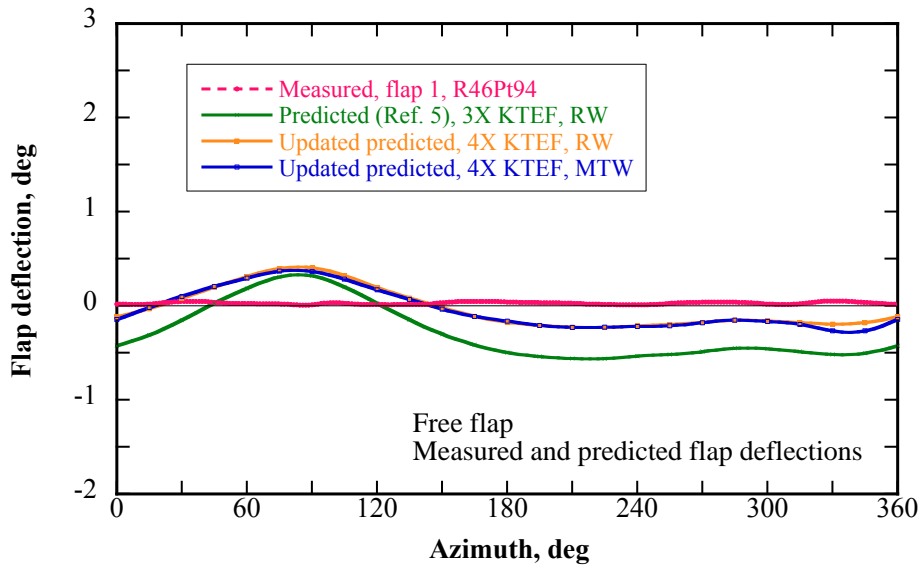
Fig. 4a. Measured and predicted flap deflections, free flap.

Fig. 4b. Torsion moment correlation, 0.64R, free flap.

American Institute of Aeronautics and Astronautics
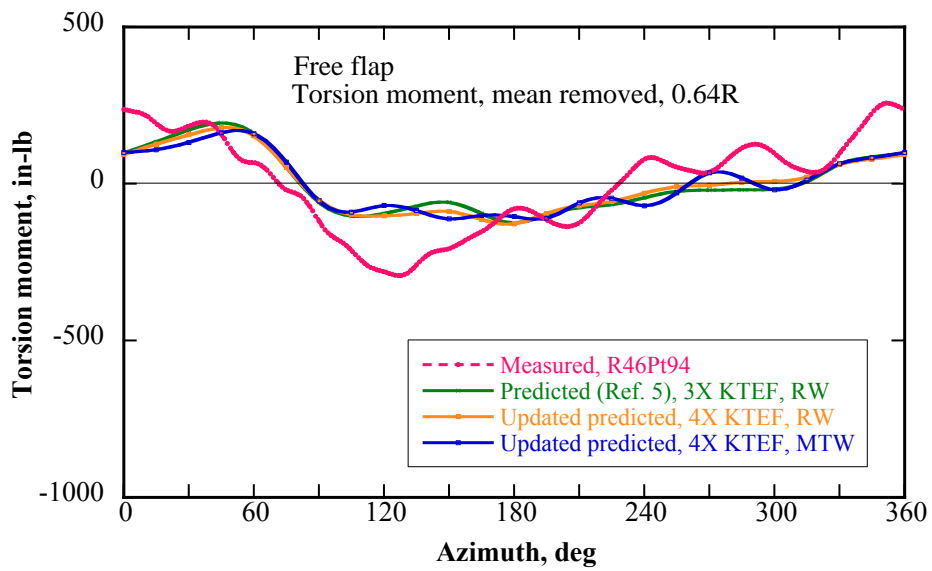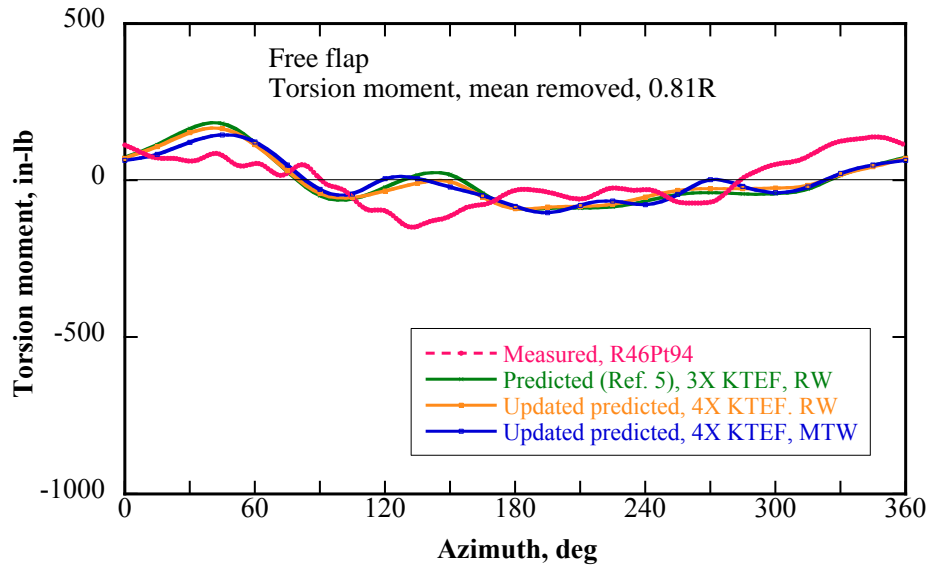
Fig. 4c. Torsion moment correlation, 0.81R, free flap.
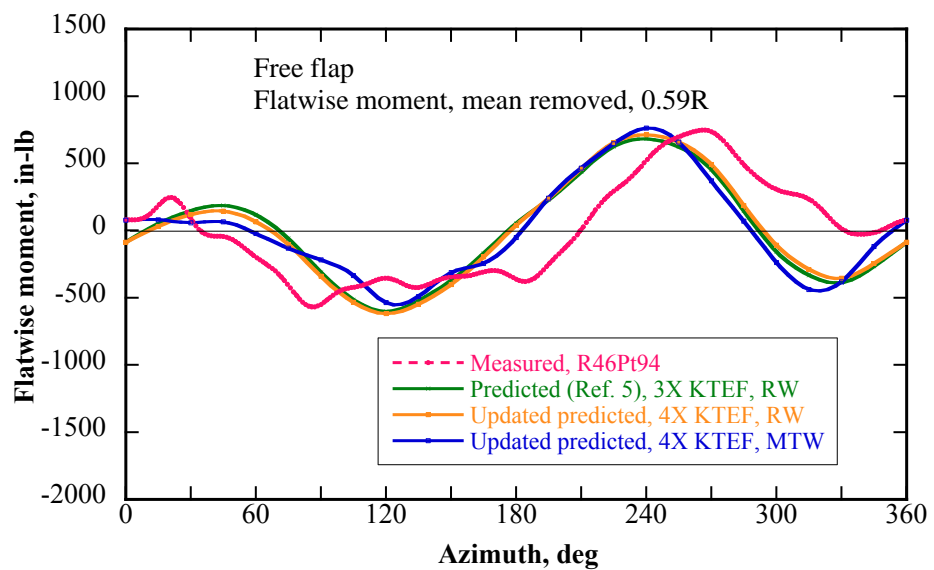
Fig. 4d. Flatwise bending moment correlation, 0.59R, free flap.
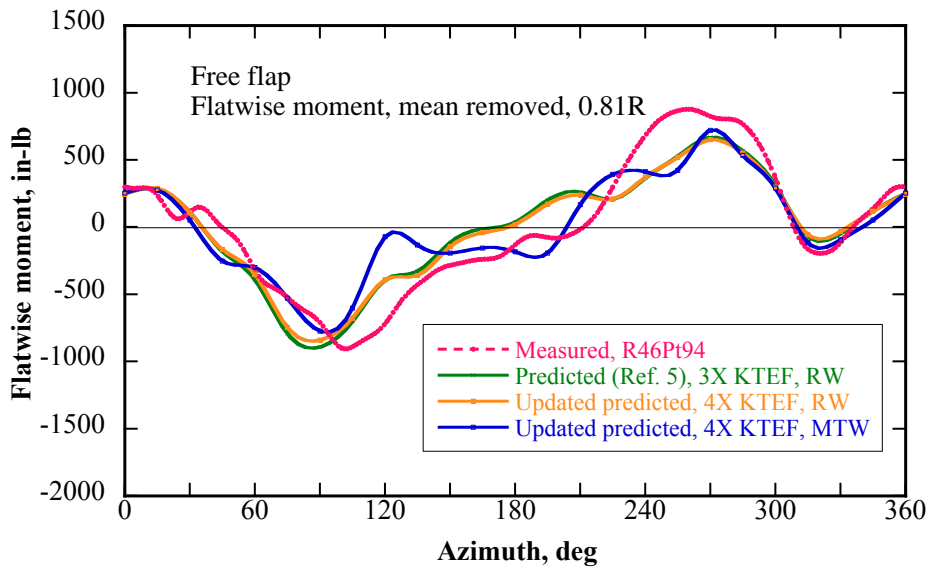
Fig. 4e. Flatwise bending moment correlation, 0.81R, free flap.

Fig. 4f. Chordwise bending moment correlation, 0.59R, free flap.

29
American Institute of Aeronautics and Astronautics
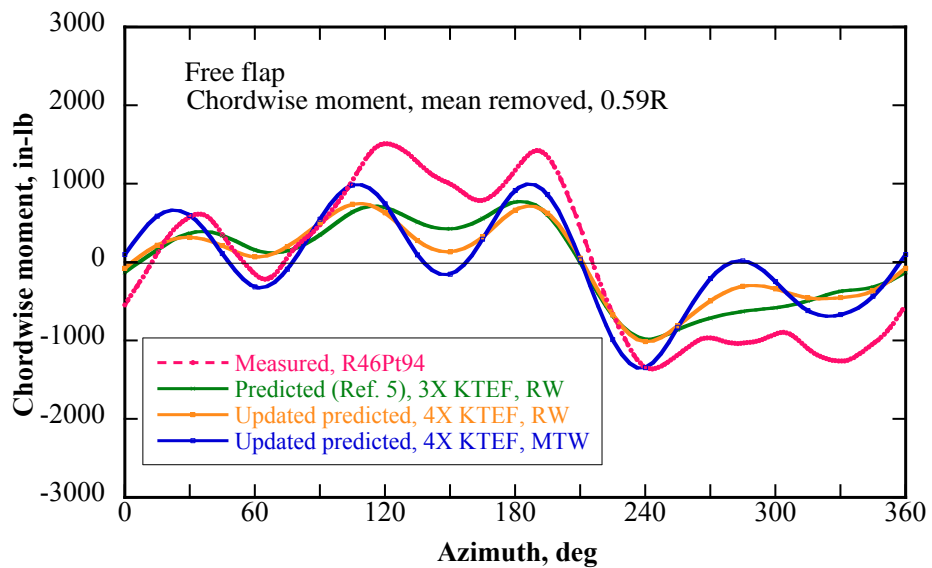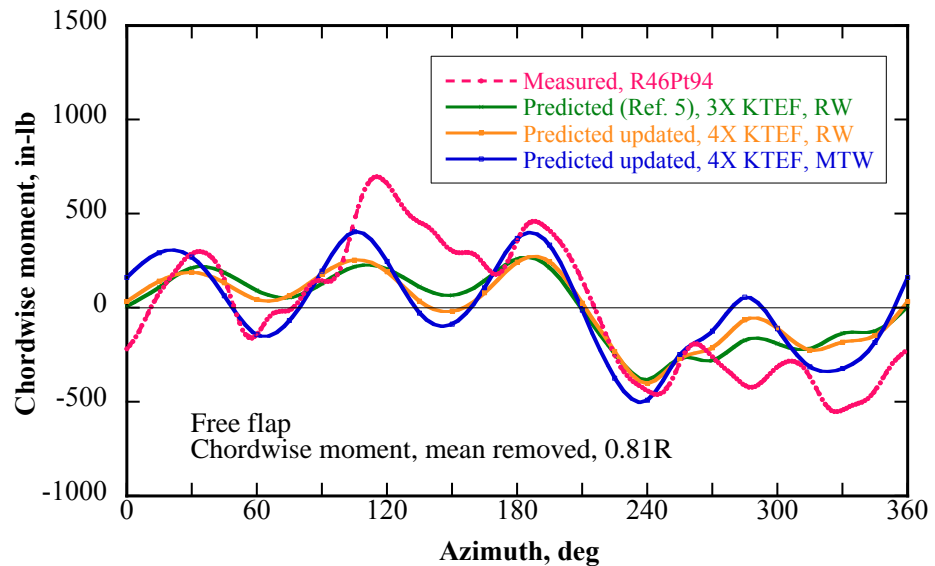
Fig. 4g. Chordwise bending moment correlation, 0.81R, free flap.
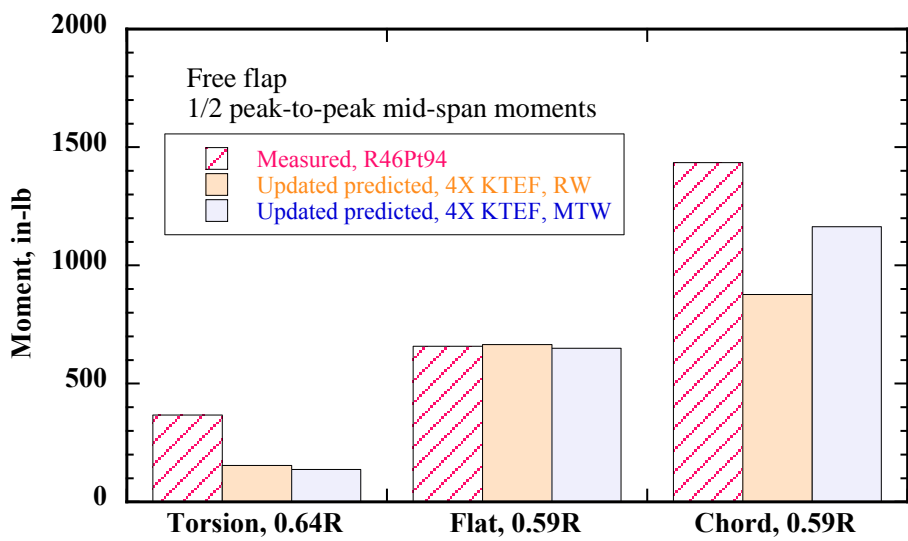
Fig. 4h. Mid-span moment correlation, free flap.

American Institute of Aeronautics and Astronautics
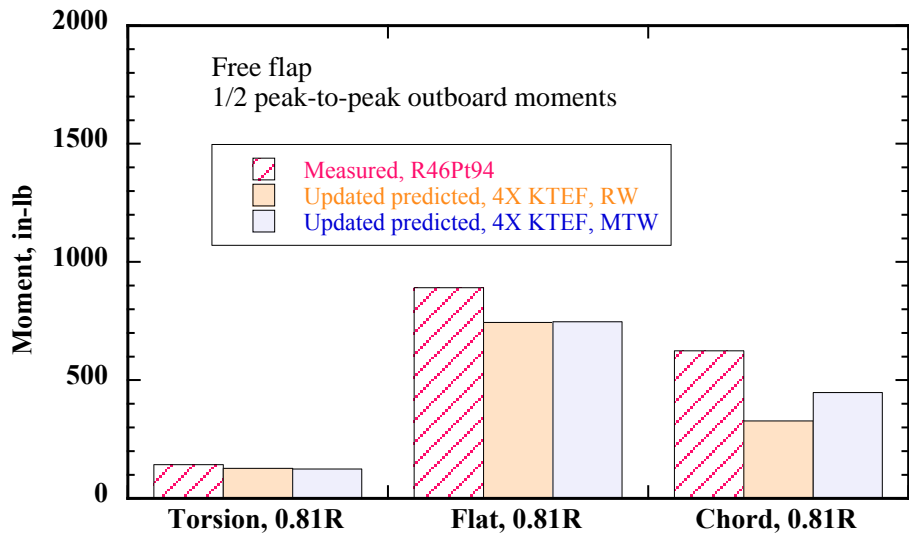
Fig. 4i. Outboard moment correlation, free flap.
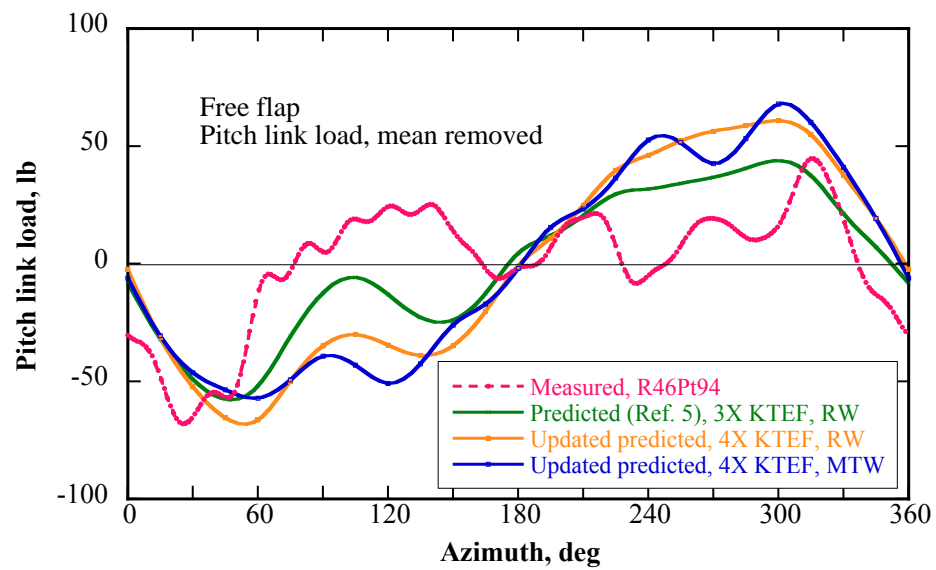
Fig. 4j. Pitch link load correlation, free flap.

American Institute of Aeronautics and Astronautics
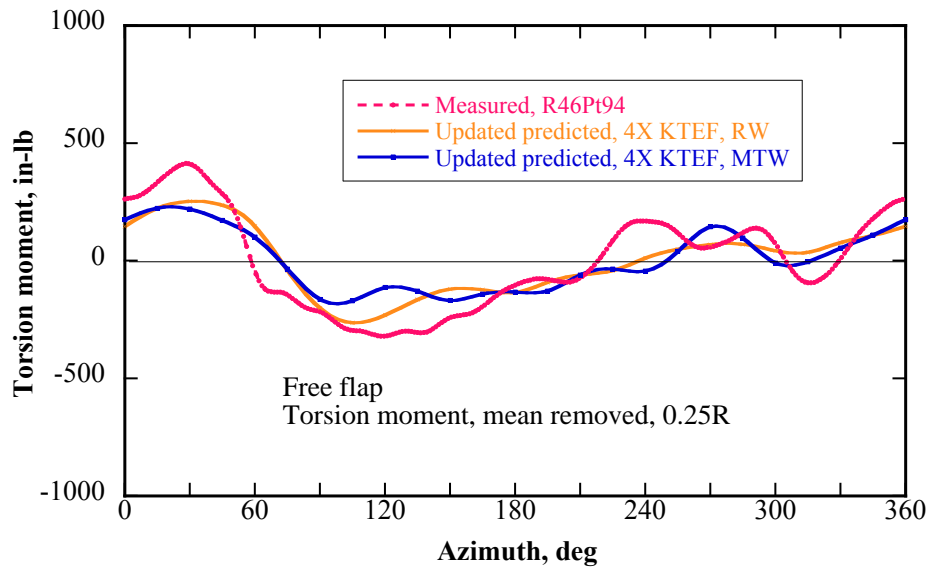
Fig. 4k. Inboard torsion moment correlation, 0.25R, free flap.
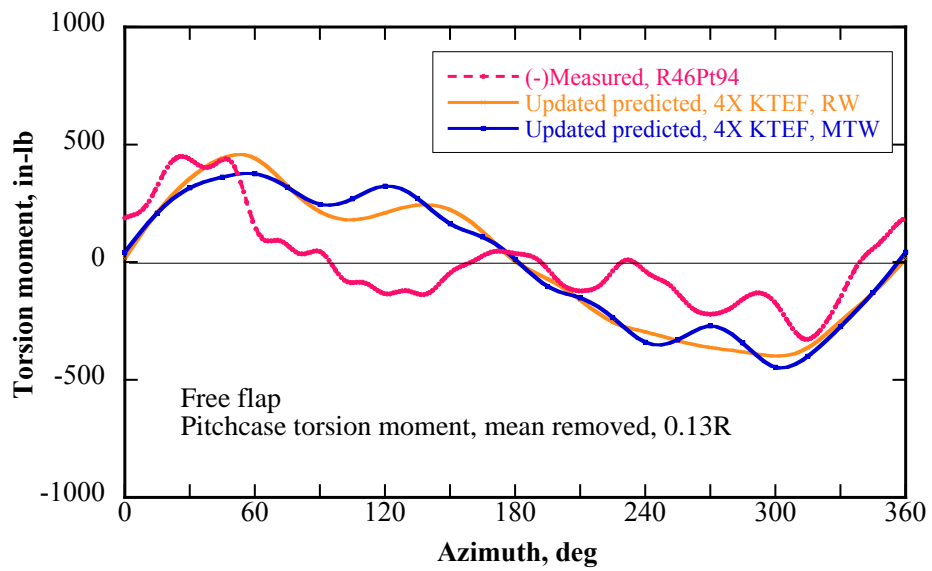
**Fig. 4l. Pitchcase torsion moment correlation, 0.13R, free flap.**
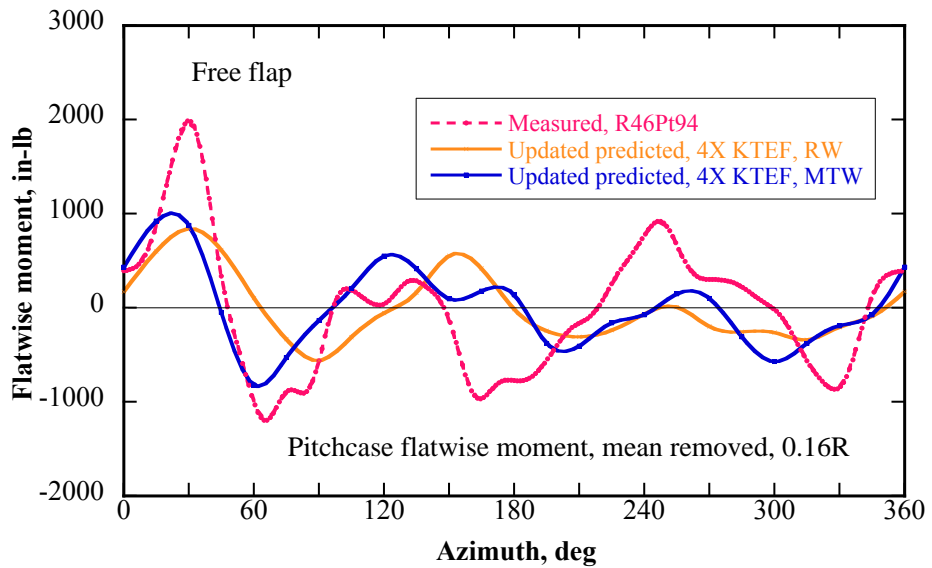
**Fig. 4m. Pitchcase flatwise moment correlation, 0.16R, free flap.**

Fig. 4n. Pitchcase chordwise moment correlation, 0.16R, free flap.

American Institute of Aeronautics and Astronautics
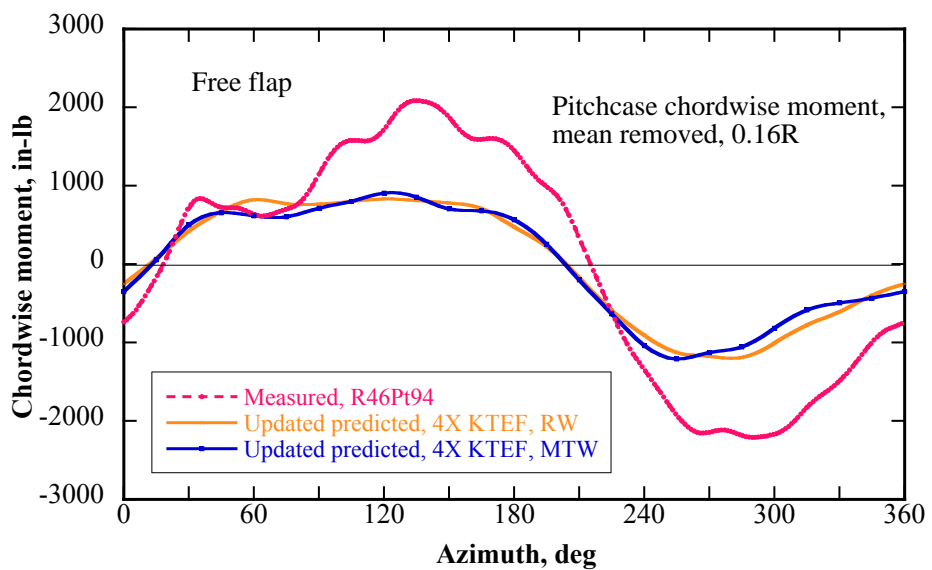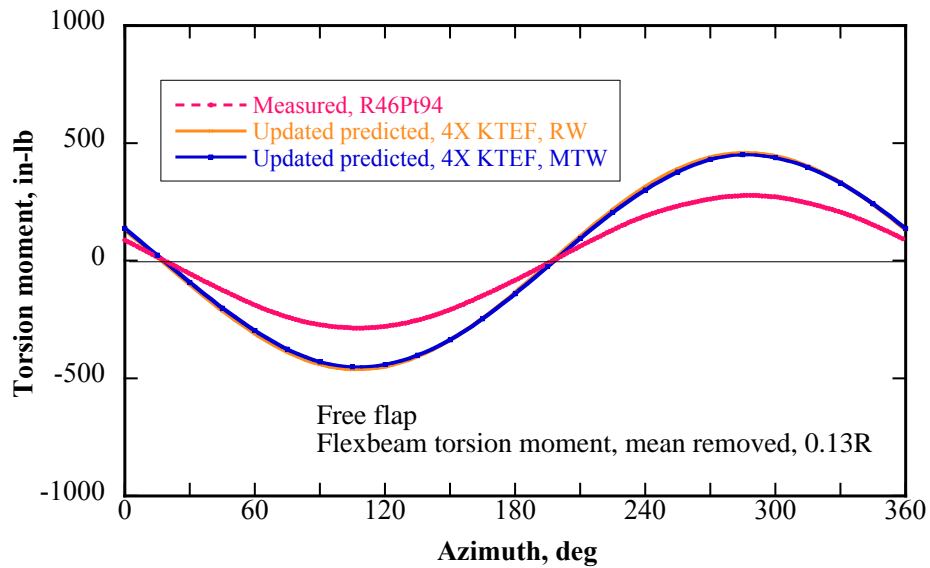
**Fig. 4o. Flexbeam torsion moment correlation, 0.13R, free flap.**

Fig. 4p. Flexbeam chordwise moment correlation, 0.13R, free flap.

American Institute of Aeronautics and Astronautics